GEOLOGICA CARPATHICA, 2025, 76, 6, 391–416 https://doi.org/10.31577/GeolCarp.2025.23

Maximum depositional age, provenance, and paleogeographic evolution of the Early Paleozoic succession of the Istanbul Zone: Insights from detrital zircon U–Pb geochronology and geochemistry

ISAK YILMAZ[1,✉], GÖKSEL DURSUN[1], SERDAR AKGÜNDÜZ[1], DAVUT LAÇIN[1], FATMA ŞIŞMAN TÜKEL[1] and BEYZANUR SERT[1]

[1]Istanbul University–Cerrahpasa, Faculty of Engineering, Department of Geological Engineering, Avcilar, Istanbul, Turkey

(Manuscript received September 17, 2025; accepted in revised form November 26, 2025; Associate Editor: Igor Broska)

Abstract: The Early Paleozoic succession of the Istanbul Zone begins with fine-grained, laminated subtidal–marine sediments containing glauconite and shallows upward into fluvial–deltaic coarse clastics. This regressive succession, continuously deposited until the Mid-Silurian transgressive phase, reaches ~3500 m in thickness. Detrital zircon U–Pb geochronology (n=513) demonstrates that deposition did not commence in the Cambrian/Precambrian but in the Ordovician, with fluvial–deltaic sedimentation of the Kurtköy Formation beginning in the Late Ordovician and continuing into the Early Silurian (Llandoverian). Whole-rock geochemistry (major and trace element discriminants such as DF1–DF2, SiO_2–Al_2O_3/TiO_2, Th/Sc–Zr/Sc, Co/Th–La/Sc) indicates that sedimentation was dominated by felsic continental crustal sources, with subordinate mafic input. Samples from the Kurtköy Formation further record back-arc/rift influence in tectonic discrimination diagrams. Provenance signals are characterized by strong Pan-African/Cadomian (750–550 Ma) contributions, along with limited Mesoproterozoic, Paleoproterozoic, and rare Archaean zircons, all pointing to a Gondwanan affinity. Paleotectonically, the succession reflects an active continental margin–arc setting during the Ordovician, with sedimentation continuing from Mid-Silurian onwards under passive margin conditions during the transgressive phase. Taken together, the chronological and geochemical data suggest that the Istanbul Zone represents an active margin basin along the northern Gondwana margin, later positioned along the easternmost part of the Armorican domains within the Galatian superterrane with the opening of the Paleo-Tethys, and ultimately accreted to Laurussia during the Variscan orogeny.

Keywords: detrital zircon U–Pb, Istanbul Zone, maximum depositional age, Ordovician–Silurian, provenance

Introduction

The Paleozoic era represents a critical interval in the geological evolution of Turkey (Türkiye), reflecting a complex interplay of continental margin dynamics, sedimentary basin development, and later tectonothermal overprinting (Fig. 1). In the Alpine orogenic framework of Turkey, most Paleozoic successions (particularly those in the Central Taurides and Eastern Anatolia) have undergone moderate to high-grade metamorphism, which significantly obscures their original depositional features (Göncüoğlu 1997; Topuz et al. 2004; Okay et al. 2008). These units typically exhibit polyphase deformation and greenschist- to amphibolite-facies metamorphic imprints, and in places are structurally stacked within large metamorphic massifs (e.g., the Menderes and Bitlis complexes; Okay et al. 1985; Whitney & Bozkurt 2002; Oberhänsli et al. 2010, 2013; van Hinsbergen et al. 2010; Heineke et al. 2019).

By contrast, the Istanbul Zone in northwestern Turkey preserves an exceptionally well-preserved, unmetamorphosed to weakly metamorphosed Lower Paleozoic sedimentary succession (Okay et al. 1994; Moix et al. 2008; Ustaömer et al. 2011). This zone forms a peri-Gondwanan fragment that was later accreted to Laurussia (Şengör & Yılmaz 1981; Bozkurt et al. 2008; Okay & Nikishin 2015) and provides a rare window into passive margin sedimentation during the Ordovician to Carboniferous along the northern margin of Gondwana (Göncüoğlu 1997; Görür et al. 1997; Göncüoğlu & Kozur 1998; Göncüoğlu et al. 2000). It has been reported that the lithostratigraphic succession of the Istanbul zone comprises quartz-rich fluvial and shallow-marine sandstones of Late Cambrian–Ordovician age, Silurian black shales and fossiliferous carbonates, and transgressive marine limestones and siltstones of Devonian age (Dean et al. 2000; Sayar & Cocks 2013).

The provenance, tectonic setting, and paleogeographic evolution of these sediments have been the subject of ongoing debate. Global paleogeographic reconstructions place the Istanbul Zone as a peri-Gondwanan continental fragment located along the northern margin of Gondwana (Stampfli & Borel 2002; Sayar & Cocks 2013; Stampfli et al. 2013; Torsvik & Cocks 2013; von Raumer et al. 2015). Local geochronological data, however, provide more direct constraints:

✉ corresponding author: Isak Yilmaz
iyilmaz@iuc.edu.tr

CC BY NC ND

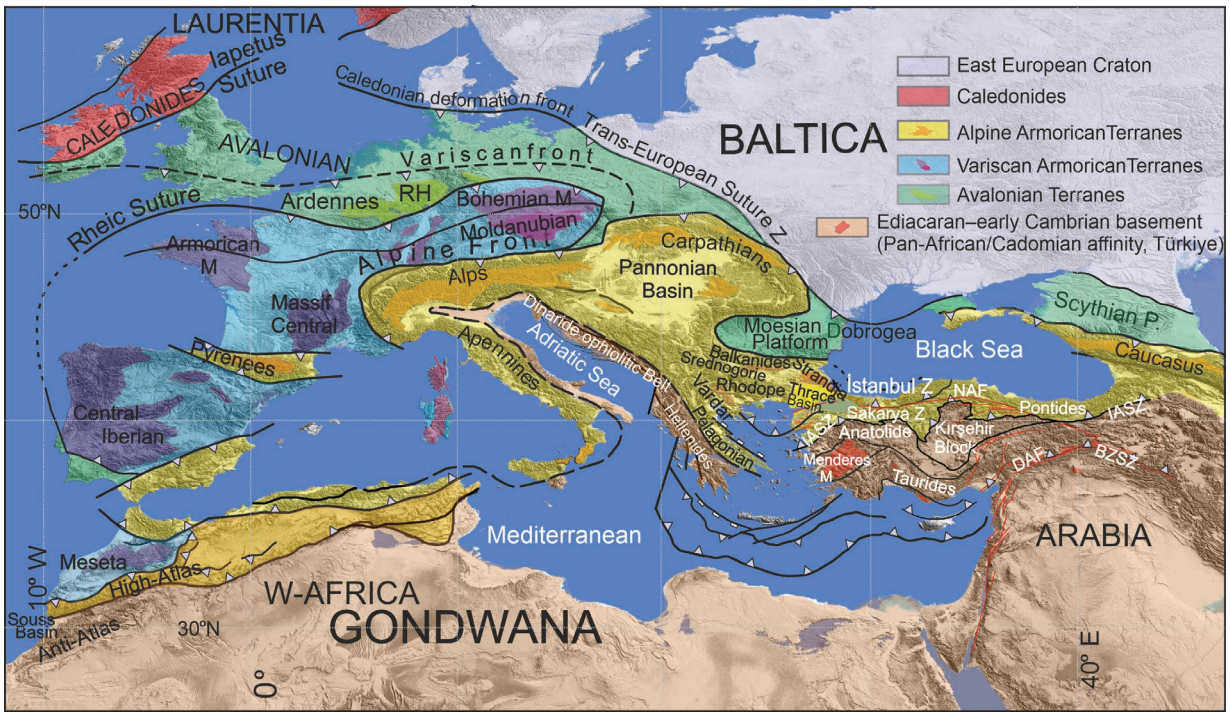


Fig. 1. Simplified tectonic framework of Europe and surrounding areas, showing the Laurentia, Baltica, Gondwana, and Peri-Gondwanan terranes during the Early Paleozoic. Avalonian, Armorican, and related peri-Gondwanan terranes are shown together with the Caledonian and Variscan deformation fronts and the Alpine suture zones (modified after Neubauer & Handler 2000; McCann 2008; Okay et al. 2008; Sharkov et al. 2012; Castillo et al. 2022). Thick black lines represent major suture zones (e.g., Tornquist Suture, Rheic Suture), whereas dashed lines indicate the Caledonian and Variscan deformation fronts. Abbreviations: RH – Rhenohercynian Zone, M – Moldanubian Zone, P – Pontides, NAF – North Anatolian Fault, DAF – East Anatolian Fault, BSZ – Bitlis Suture Zone, IASZ – Izmir–Ankara Suture Zone.

zircon U–Pb ages from the basement granitoids in Bolu (Ustaömer et al. 2005) and basement units in Safranbolu (Chen et al. 2002) confirm the presence of a Pan-African/Cadomian-affiliated basement. Furthermore, detrital zircon age spectra from Lower Ordovician quartzites indicate a Gondwanan provenance and suggest a possible Amazonian contribution (Ustaömer et al. 2011). Based on paleomagnetic data, Öksüm et al. (2015) proposed that the Istanbul Zone rifted away from a location close to Amazonia during the Early Ordovician and was transported eastward along the equatorial belt by dextral strike-slip motion throughout the Silurian–Devonian. More recent zircon U–Pb–Hf studies have reinforced this Gondwanan link and highlighted possible correlations with Avalonia (Akdoğan et al. 2021; Şen 2023; Yılmazer et al. 2024, 2025). On the other hand, paleontological and stratigraphic evidence suggest similarities between the Istanbul Zone and Avalonia as well as Armorica (Yanev et al. 2006; Bozkurt et al. 2008). Moreover, the absence of Variscan metamorphic overprint and the relatively continuous Paleozoic stratigraphy distinguish the Istanbul Zone from neighboring tectonostratigraphic units such as the Sakarya Zone and the Central Pontides (Okay et al. 2008; Moix et al. 2008).These interpretations are drawn from previous studies and are presented here to contextualize the ongoing debate; they do not reflect the new results of this study regarding the maximum depositional age and paleogeographic evolution of the Istanbul Zone, and the same applies to the geological background summarized in the following section.

Understanding the sedimentary evolution of the Istanbul Zone during the Early Paleozoic is key to reconstructing both the regional paleogeography of peri-Gondwana and the broader geodynamic context of the northern Gondwanan margin. In particular, identifying the sediment sources, chemical weathering intensity, and paleoclimatic regime during deposition offers crucial insights into plate-margin evolution, ocean opening processes, and continental dispersal mechanisms in the Early Paleozoic (Nance & Murphy 1996; von Raumer & Stampfli 2008). Moreover, the preservation of primary sedimentary and geochemical signatures within the Istanbul Zone allows for the application of integrated analytical techniques to address these questions.

In summary, the literature emphasizes that the main criteria distinguishing the Istanbul Zone from adjacent tectonostratigraphic units are the presence of a Cadomian/Pan-African basement, stratigraphic continuity, and the absence of a pronounced Variscan overprint; within this framework, the zone is treated as a key reference for reconstructing peri-Gondwanan paleogeography. The onset of sedimentation has been variably interpreted among studies – Ordovician in some (Sayar 1964; Önalan 1981; Dean et al. 2000; Ustaömer et al. 2011; Özgül 2012), Cambrian in others (Boztuğ 1992; Sayar & Cocks 2013; Yılmazer et al. 2025), and even Precambrian

(Şen 2023). A similar spread exists in paleogeographic interpretations: many models relate the zone to Avalonia or Amazonia, invoking rifting from the northwestern margin of Gondwana and accretion to Baltica – followed by incorporation into Laurussia – early in the Paleozoic.

The primary aim of this study is to evaluate the detrital zircon U–Pb age data and geochemical analyses of sandstones from the Lower Paleozoic clastic succession of the Istanbul Zone in order to constrain their depositional age, provenance characteristics, and paleogeographic setting. In this framework, zircon age spectra provide insights into the timing of deposition and contributions from multiple continental sources, whereas major and trace element geochemistry offers additional constraints on weathering intensity, paleoclimatic conditions, and tectonic environment. The new geochronological and geochemical data presented in this study directly contribute to these debates and allow for a reassessment of the Early Paleozoic evolution of the Istanbul Zone.

Geological setting of the Istanbul Zone during the Early Paleozoic

The Istanbul Zone is a peri-Gondwanan continental fragment located along the southwestern margin of the present-day Black Sea, and it records a complex geological evolution shaped by Precambrian basement development, Paleozoic sedimentation, and Mesozoic–Cenozoic tectonic processes. It is bounded by the Rhodope–Strandja Zone to the west, the Sakarya Zone to the south, and the Black Sea to the north (Okay et al. 1994; Bozkurt et al. 2008; Akdoğan et al. 2021; Yılmazer et al. 2025). Structurally, the zone is delineated by major tectonic features such as the Western Black Sea Fault and the active North Anatolian Fault (NAF). To the south, the Istanbul Zone is separated from the Sakarya Zone by the Intra-Pontide Suture Zone (IPSZ), which is transected by the NAF. The IPSZ has been interpreted in some studies as a remnant of the Neo-Tethyan suture (Şengör & Yılmaz 1981; Okay & Tüysüz 1999; Marroni et al. 2020), whereas other interpretations suggest that it represents a Carboniferous suture corresponding to the Rheic domain (Okay & Topuz 2017; Akdoğan et al. 2021).

The pre-Cretaceous configuration of the Istanbul Zone suggests that it was originally located along the Odessa Shelf on the southern margin of the East European Platform, adjacent to the Moesian Platform. Its southward translation to its present location was driven by the Late Cretaceous back-arc opening of the Western Black Sea Basin (Okay et al. 1996, 2018). Stratigraphic similarities between the Istanbul Zone and the Moesian Platform, as revealed through drill cores and seismic data, support this hypothesis (Nikishin et al. 2015).

The basement of the Istanbul Zone consists of a Late Neoproterozoic crystalline complex, composed of high-grade amphibolite-facies rocks (gneiss, amphibolite, and migmatites), disrupted meta-ophiolites (including metagabbro and metaperidotite), and metavolcanic–metasedimentary assemblages intruded by voluminous granitoids. U–Pb zircon ages from these intrusives range from 590 to 560 Ma, consistent with arc-related Cadomian magmatism (Chen et al. 2002; Ustaömer et al. 2005). The Bolu Massif represents the largest exposure of this basement and has been interpreted as part of an accreted oceanic arc based on geochemical, lithological, and isotopic evidence (Yılmazer et al. 2025).

The Paleozoic sedimentary cover, more than 5 km thick, unconformably overlies the basement and spans from the Early Ordovician to the Late Carboniferous (Dean et al. 2000; Okay et al. 2006). The succession begins with fluvial conglomerates and sandstones, overlain by shallow-marine quartzites of Tremadoc–Arenig age, followed by Middle Ordovician mudstones and shales. The Silurian sequence comprises graptolite-bearing black shales and shallow marine carbonates, passing upward into fossiliferous Devonian siltstones, shales, and limestones (Fig. 2). This evolution reflects the transition from continental to progressively deeper marine environments (Haas 1968; Önalan 1981; Özgül 2012; Sayar & Cocks 2013).

Stratigraphic, paleontological, and radiometric studies on the basin evolution predating the Aydos Formation quartzites have variously proposed that the underlying clastic succession began as early as the Cambrian (Boztuğ 1992; Sayar & Cocks 2013; Yılmazer et al. 2024), or even the Precambrian (Şen 2023), whereas other studies place its onset in the Ordovician, including the deposition of the Aydos quartzites (Ustaömer et al. 2011; Özgül 2012). One of the earliest comprehensive works on the geology of Istanbul, Paeckelmann's monograph "Geologie Thraziens, Bithyniens und der Prinzeninseln" (1938), presented a different interpretation. Based on stratigraphic observations, Paeckelmann described this thick clastic sequence as the "Hauptkonglomerat und Arkose-Horizont" and assigned it to the Wenlock–Ludlow interval (Middle–Upper Silurian) based on lithostratigraphic correlation with Silurian clastic sequences of the Thrace–Bithynia region rather than direct paleontological evidence.

In the eastern part of the zone (e.g., Zonguldak and Çamdağ regions), the Silurian is often absent or significantly reduced, and the Devonian begins with a marked angular unconformity overlying Tremadocian siliciclastics. The absence of Variscan deformation and the presence of low CAI values in conodonts (CAI=1–2.5) in Devonian–Carboniferous units suggest that the Istanbul Zone remained tectonically quiescent throughout most of the Paleozoic (Göncüoğlu & Kozur 1998; Moix et al. 2008). This contrasts with more intensely deformed regions south of the IPSZ, such as the Sakarya Zone (Okay & Tüysüz 1999).

Geochemical and isotopic studies indicate that the basement of the Istanbul Zone shares affinities with the Pan-African basement of northern Gondwana, implying a peri-Gondwanan origin (Okay et al. 2008). Ustaömer et al. (2011) reported that detrital zircon U–Pb age spectra from Ordovician quartzites are dominated by Late Neoproterozoic to Early Paleozoic populations, and Yılmazer et al. (2025) stated that the εHf(t) values of sandstones from the Bolu and Karadere areas indicate the presence of both juvenile and crustal components.

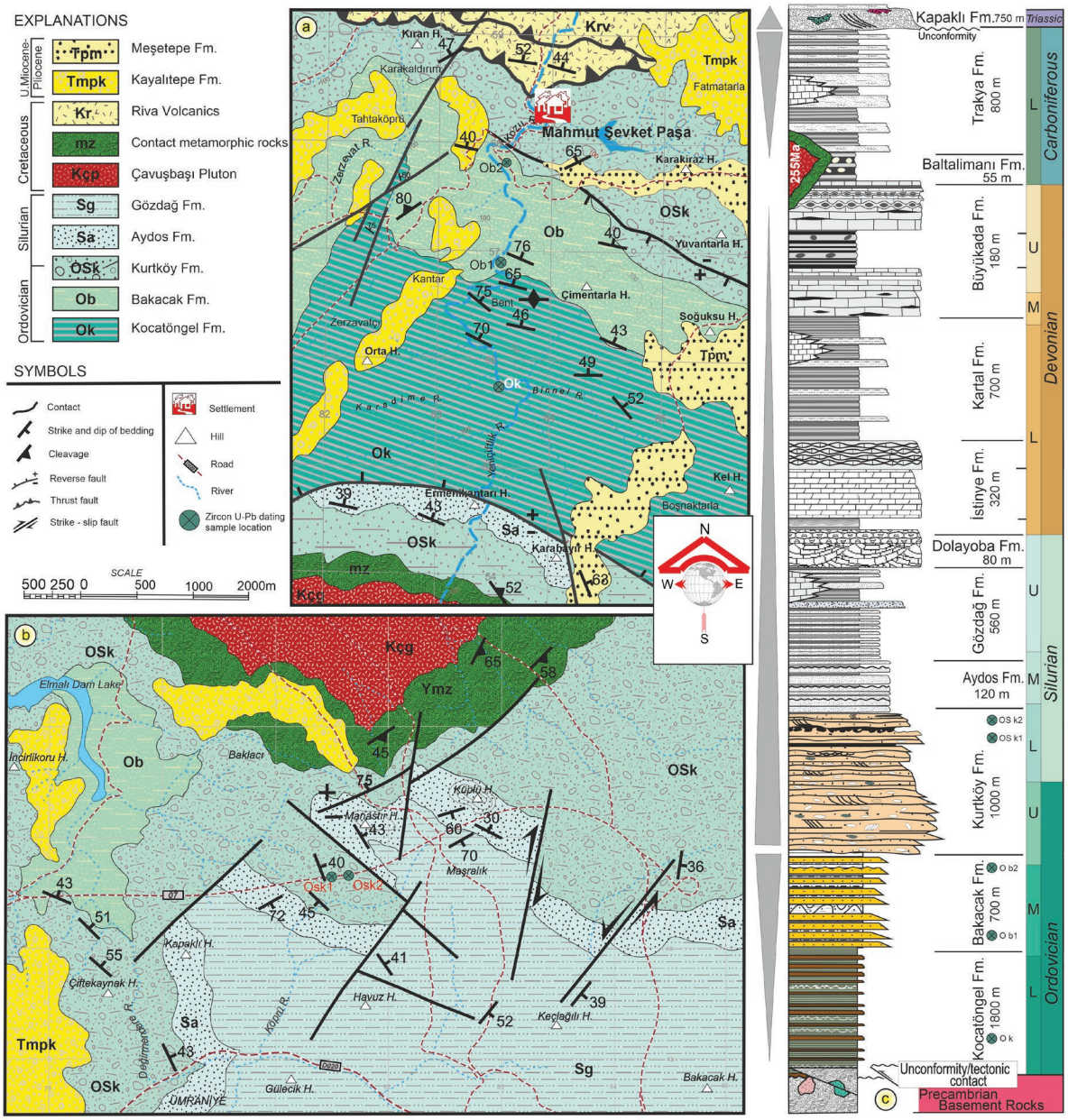


Fig. 2. a, b — Geological maps of the areas within the Early Paleozoic succession of the Istanbul Zone where geochronological and geochemical samples were collected. **c** — Generalized stratigraphic column of the Paleozoic succession of the Istanbul Zone.

Ustaömer et al. (2011) further emphasized that Amazonian signatures within the detrital zircon assemblages point to sediment derivation from the northwestern margin of Gondwana.

It has been proposed that the stratigraphic continuity, limited deformation, and fossil assemblages of the Istanbul Zone indicate an Atlantic-type passive continental margin setting (Okay 1989; Görür et al. 1997). This passive-margin configuration is suggested to have persisted from the Ordovician to the Carboniferous, with the onset of sedimentation beginning in the earliest Ordovician (Dean et al. 2000). Previous studies further demonstrated that the entire Paleozoic succession was deformed during the Late Carboniferous, developing northeast-vergent folds and thrusts (Zabcı et al. 2003; Okay et al. 2008), and was subsequently intruded by Middle–Upper Permian granitoids (~255 Ma) (Yılmaz 1977; Aysal et al. 2018).

Methodology

The Early Paleozoic clastic succession of the Istanbul Zone has, until now, remained analytically underexplored in terms of both depositional ages and source rock characteristics, largely due to the scarcity of fossil evidence in the lower and middle parts of the succession. As a result, previous

stratigraphic interpretations have relied primarily on sedimentological observations and limited lithostratigraphic correlations (Dean et al. 1997; Bozkaya et al. 2002). To date, analytical data from this succession have been restricted to paleomagnetic results and detrital zircon U–Pb dating of quartz sandstones from the overlying Aydos Formation (Ustaömer et al. 2011; Öksüm et al. 2015). In contrast, this study presents, for the first time, detailed geochemical and geochronological analyses of the ~3500 m-thick, fine-grained laminated regressive succession underlying the transgressive deposits of the Aydos Formation, together with the overlying terrestrial, red-colored coarse-grained fluvial sediments. This has enabled much stronger inferences regarding the timing of deposition, the evolution of sediment sources, and the geodynamic setting of the succession.

As part of this study, extensive fieldwork was conducted along different segments of the ~400 km-long succession exposed across the Istanbul Zone. Facies characteristics, structural positions, and stratigraphic continuities of the sedimentary units were examined in detail. Geochemical, petrographic, and geochronological analyses were performed on representative samples selected from the most continuous and well-measured sections, ensuring high sampling reliability. Within the Istanbul metropolitan area, two key outcrop regions on the Anatolian side were targeted, with a particular focus on the Beykoz district in the west, where wider exposures occur (Fig. 2a,b).

Representative samples of fine-grained, laminated marine deposits at the base of the succession (Kocatöngel and Bakacak formations) were collected from the Yeniçiftlik Stream valley flowing south toward Mahmut Şevket Paşa village. Red-colored, coarse-grained terrestrial facies (Kurtköy Formation) from the upper part of the succession were sampled from a road cut along the Çekmeköy–Beykoz district boundary.

In total, petrographic analyses were conducted on sixty representative samples, complemented by XRD measurements, and geochemical analyses were performed on twenty-five samples. Furthermore, detrital zircon U–Pb dating was carried out on 571 grains randomly selected from five samples, including three from the fine-grained basal units (Kocatöngel and Bakacak formations) and two from the coarse-grained upper units (Kurtköy Formation).

This sampling strategy provides the first comprehensive evaluation of both the geochemical characteristics and zircon age spectra of the regressive marine succession and the overlying terrestrial deposits.

X-ray diffraction (XRD) analysis

To determine the mineralogical composition of selected samples, XRD analysis was performed. Representative samples were dried at 60 °C for 16–18 hours, pulverized, and sieved to <80 mesh. Measurements were conducted at the Department of Mineralogy–Petrography, Faculty of Engineering, Istanbul University–Cerrahpaşa, using a GNR APD Pro–2000 diffractometer operating with Cu Kα radiation, Ni filter, 40 kV voltage, and 30 mA current. The scan was performed at a goniometer speed of 1° 2θ/min with a sensitivity of 1 cm/min. Resulting diffractograms were interpreted using the Philips High Score Plus software and compared with JCPDS reference cards to identify mineral phases.

Whole-rock geochemical analyses

Bulk-rock geochemical analyses were conducted to determine the major, trace, and rare earth element concentrations of representative sandstone and siltstone samples from the Early Paleozoic siliciclastic succession in the Istanbul Zone. Rock samples were initially crushed using a jaw crusher and pulverized with a disc mill to obtain homogeneous powder. To assess volatile components, Loss on Ignition (LOI) was calculated by heating the samples at 950 °C for two hours. Following LOI, samples were digested using strong acid mixtures (e.g., HF–HNO_3 or aqua regia) based on standard geochemical protocols. The resulting solutions were diluted to appropriate concentrations for instrumental analysis.

Major element concentrations were measured using a PerkinElmer Avio 200 ICP–OES instrument, and trace and rare earth elements were quantified using a PerkinElmer NexION 2000 ICP–MS system, both housed at the Geochronology and Geochemistry Laboratory of Istanbul University–Cerrahpaşa (IUC-GGL). Data were interpreted using the GCDKit software package, allowing evaluation of elemental distributions, normalization diagrams, and geochemical discrimination plots to assess rock types, alteration levels, and possible source characteristics.

U–Pb zircon geochronology

To constrain the depositional age and provenance of the clastic units, detrital zircon U–Pb dating was performed on selected samples. Zircon grains were separated from bulk sediment by dry sieving into 63 µm and 125 µm fractions, followed by Wilfley table concentration, Frantz magnetic separation, and heavy liquid separation using bromoform (ρ>2.9 g/cm^3). Zircons were hand-picked under a binocular microscope, mounted in epoxy, and polished to expose internal structures.

Grains were imaged using transmitted light and cathodoluminescence to reveal zoning and internal morphology, which guided spot selection. U–Pb isotopic analyses were conducted at IUC-GGL using a NexION 2000B ICP–MS coupled with an ESI New Wave NWR-213 solid-state laser ablation system. Analytical conditions included a spot size of 25–40 µm (adjusted based on internal grain texture), laser energy of 5 J/cm^2, and a repetition rate of 5 Hz. Helium (0.5 L/min) was used as the carrier gas. The zircon standard 91500 (1065±2 Ma; Wiedenbeck et al. 2004) was used as the primary reference, with AusZ-10 (38.6 Ma; Kennedy et al. 2014) and MudTank (730±12 Ma; Black & Gulson 1978) as secondary standards. Data reduction was carried out using the Iolite Software v2.5 (Paton et al. 2011) for peak integration and

isotope ratio calculation, and IsoplotR (https://isoplotr.es.ucl.ac.uk/) was used for age computation. Concordance levels were evaluated, and concordia diagrams were used to determine crystallization ages and infer the possible magmatic or metamorphic origin.

Maximum depositional ages (MDA) were determined from the youngest concordant $^{206}Pb/^{238}U$ ages of detrital zircons. We applied multiple approaches commonly used in detrital zircon geochronology (Vermeesch 2012; Gehrels 2014): (i) the youngest single grain (YSG), (ii) the youngest coherent cluster of at least two overlapping ages at 2σ uncertainty (YC2σ), and (iii) the weighted mean of the youngest population where applicable. For comparison, we also tested the TuffZirc algorithm (Ludwig 2003), which statistically identifies the youngest coherent population. All approaches yielded consistent results within uncertainty, confirming the robustness of the depositional age constraints. Reported MDA values are based primarily on YSG and YC2σ, with TuffZirc results provided as supportive evidence.

Results

Stratigraphy and sedimentary features of the Early Paleozoic Istanbul Zone

In the east–west–trending Istanbul Zone, the Lower Paleozoic succession is represented by clastic units that reflect changing depositional conditions through time, yet laterally display comparable facies and lithological characteristics along the zone. The succession developed as a result of the Silurian transgressive episode is unconformably overlain by Permo–Triassic basal conglomerates. In the western parts of the zone, this transgression continued uninterrupted until reaching deep-marine conditions in the Carboniferous, whereas in the eastern areas, deposition occurred more locally within restricted domains between land and shelf, with interruptions such as during the Silurian–Devonian transition (Sayar 1964; Arpat et al. 1978; Önalan 1981; Dean et al. 1997, 2000; Göncüoğlu & Kozur 1998, 1999; Göncüoğlu & Kozlu 2000; Gedik et al. 2002; Yanev et al. 2006; Yalçın & Yılmaz 2010; Sachanski et al. 2012).

At the base of the succession, the deposits are 1500–1800 m thick and consist of monotonous greenish-grey, grey, and dark ash-colored strata. These include well-developed parallel-laminated, varve-like successions that locally exhibit disharmonic folds, wavy and convolute structures, as well as low-angle and hummocky cross-laminations (Fig. 2c). This unit, defined as the Kocatöngel Formation, shows a gradual upward increase in grain size toward the sandy fraction and is composed of siltstone–mudstone alternations formed by low-energy rhythmic sedimentation, without pronounced facies transitions. The succession exhibits hard, compact argillitic characteristics, with cleavage planes crosscutting the laminations, and hosts mineral growths indicative of early diagenetic to very low-grade metamorphic conditions (Fig. 3a_1–a_3).

Within the regressive succession, the upward increase in grain size is accompanied by sand-dominated deposition, marked in the field by a color change from green at the base to reddish, greyish-pink, purple, and violet hues. This unit, defined as the Bakacak Formation and reaching thicknesses of up to 700 m, is composed of silica-cemented sandstone–shale alternations. It displays cross-lamination and oscillation ripple marks in its upper levels, reflecting shallow depositional conditions, and locally contains pebble intercalations (Fig. 3b, c). At the base, coarse-grained, locally massive, thick- to medium-bedded debris-flow deposits, including mudflow and rubble-flow facies, indicate the onset of sedimentation that later evolved into the continental deposits of the Kurtköy Formation during alluvial fan development.

These red, purple, and brown deposits are characterized by highly variable thicknesses and facies laterally, and commonly contain polygenic paraconglomerates, pebbly sandstones, sandstones, and mudstone lenses. Up-section, decreasing grain size and bed thickness mark a transition into braided- and meandering-river, floodplain, and deltaic environments, with the unit attaining a total thickness of ~1000 m. The formation is dominated by debris flows and displays pebble imbrications, planar and trough cross-bedding, and in its uppermost levels epsilon cross-bedding indicative of meandering-river environments. The succession is marked by erosional-based sequences, and sandy horizons frequently contain large, rounded mud clasts (rip-up clasts) up to pebble size, commonly in red and green colors (Fig. 3d).

Variable cross-laminations record paleocurrent directions that are predominantly southward (Önalan 1981). Particularly in the finer-grained upper levels of the succession, soft-sediment deformation structures – such as flame structures, pillows, and ball-and-pillow features – are observed at bed boundaries, reflecting earthquake-related loading processes. The Kurtköy Formation incorporates a wide variety of grains that reflect different source lithologies, ranging from low-grade metamorphic fragments to high-grade metamorphic clasts with quartz ribbons, as well as andesitic volcanic detritus and granitic pebbles.

This high-energy succession passes upward into the marine coastal deposits of the transgressive phase. These deposits consist of mature quartz sandstones in light yellow, white, and beige colors, characterized by mudcracks, NW–SE-trending ripple axes, *Cruziana* traces, vertical burrows, and *Skolithos*-type ichnofossils. Brecciated intervals and locally folded seismite horizons are also observed, a feature that is likewise common in the overlying carbonate platform strata. The transition between the Kurtköy and Aydos formations varies laterally depending on coastal morphology and sediment supply, resulting in significant differences in the thickness of coastal deposits (10–200 m) across the zone (Fig. 2).

Mineralogy and petrography

X-ray diffraction (XRD) analyses of the Kocatöngel, Bakacak, Kurtköy, and Aydos formations reveal a marked

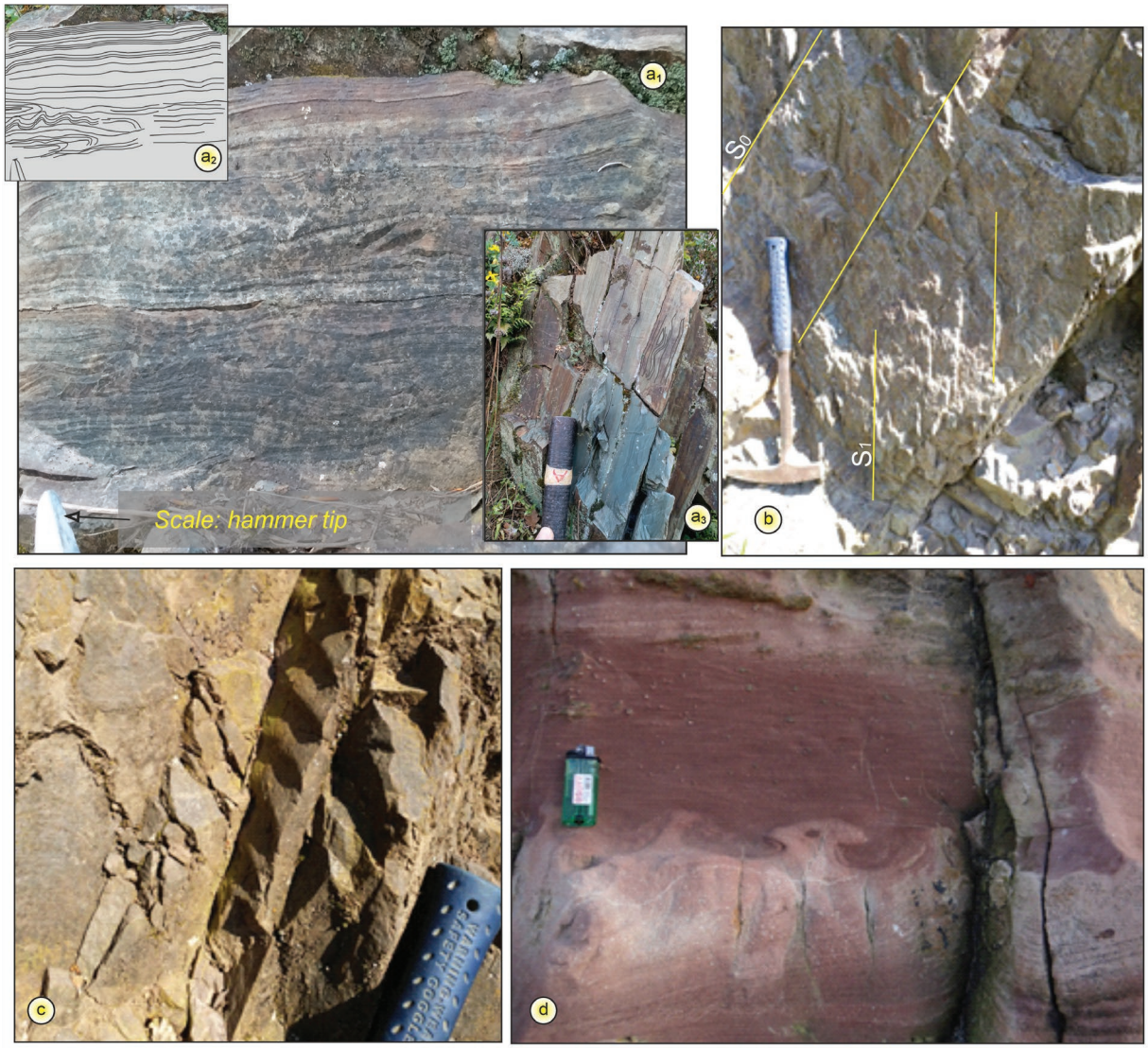


Fig. 3. Features from the basal levels of the Early Paleozoic clastic succession in the Istanbul Zone. **a** — Parallel lamination associated with slump-type soft-sediment deformation structures (irregular wavy–convolute lamination) in the laminated levels of the Kocatöngel Formation; **b** — Axial-plane cleavage developed within siltstone levels of the Bakacak Formation (a tectonic deformation structure) in Sakarya–Çamdağ; **c** — Oscillation ripples of Bakacak Formation indicating shallowing; **d** — In the upper levels of the Kurtköy Formation, cross-lamination at the base is overlain by earthquake-induced soft-sediment deformation structures, including flame, pillow, and ball structures in İstanbul/Kınalı island.

stratigraphic evolution in mineralogical composition throughout the Istanbul Zone from the Early Ordovician to the late Middle Silurian. This evolution reflects the dynamic interplay among sediment sources, climatic regimes, and depositional environments. At the base of the succession, the Kocatöngel Formation is characterized by common minerals such as illite, muscovite, chlorite, vermiculite, and albite, along with notable occurrences of glauconite and chamosite (Fig. 4). The presence of glauconite provides critical insights into the depositional environment, as this mineral forms authigenically under highly specific geochemical and physical conditions in marine settings and does not develop in freshwater lakes (Odin & Matter 1981; Amorosi 1997). Although the varve-like, finely laminated, monotonous pelitic character of the Kocatöngel Formation has occasionally been interpreted as indicating lacustrine deposition, the occurrence of glauconite undermines this interpretation and instead supports a low-sedimentation-rate, shallow marine or distal shelf environment.

This formation, which is notably rich in mineral diversity, also preserves physically and chemically unstable phases. Such preservation indicates that the sediments were rapidly buried without significant weathering, under semi-arid to temperate climatic conditions where physical weathering dominated (Nesbitt & Young 1982; Fedo et al. 1995). Stratigraphically upward, the Bakacak and Kurtköy formations show an increase in quartz and feldspar contents, while mica and

clay minerals decrease. This pattern reflects shorter transport distances, more energetic fluvial–deltaic environments, and a regime characterized by reduced source variability (Bahlburg & Dobrzinski 2011). At the top of the succession, the Aydos Formation is composed almost entirely of quartz and represents intensely weathered, highly mature sediments. The near-complete disappearance of feldspar and clay minerals indicates prolonged chemical weathering, selective transport, and repeated recycling (Taylor & McLennan 1985; Dinis et al. 2017).

Thin-section observations reveal that each formation exhibits distinct petrographic characteristics. The Kocatöngel Formation consists of quartz, plagioclase, K-feldspar, biotite, sericite, opaque minerals, olivine, and clay minerals, and contains microfractures related to cataclastic deformation. Quartz grains display undulose extinction and dendritic edge development, whereas plagioclase shows polysynthetic and contact twinning and is locally altered to sericite, epidote, and chlorite. Glauconite minerals are also present in some samples. Glauconite grains of varying sizes and morphologies exhibit distinctive optical features in both plane- and cross-polarized light. Their occurrence cutting across lamination planes indicates that they formed under authigenic conditions after deposition, rather than being deposited with the sediment. Some samples show disharmonic folds in laminae and irregular, scalloped boundaries at the contact with overlying coarse-grained units; these are interpreted as soft-sediment water-escape structures. The deformation is linked to earthquake activity (seismites), and these microscopic features are consistent with macroscopic soft-sediment deformation structures documented in the field (Fig. 5a$_1$, a$_2$).

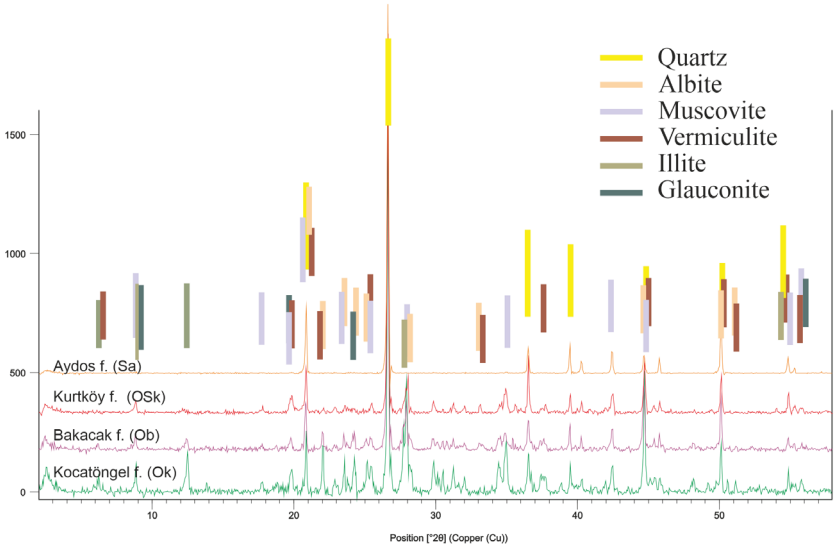


Fig. 4. XRD patterns of representative samples from the Early Paleozoic clastic succession of the Istanbul Zone (Kocatöngel Fm. – Ok, Bakacak Fm. – Ob, Kurtköy Fm. – OSk, Aydos Fm. –Sa).

Alteration has led to epidotization and chloritization. Quartz grains display undulose extinction and fracturing related to cataclastic deformation. Feldspars show contact and albite twinning, while plagioclase also exhibits polysynthetic twinning (Fig. 5b). Accessory metamorphic components such as chlorite, epidote, and garnet indicate input from metamorphic sources ranging from greenschist to amphibolite facies conditions.

The Kurtköy Formation consists of quartz, K-feldspar, plagioclase, muscovite, biotite, and metamorphic rock fragments; the metamorphic-derived grains show undulose extinction and foliated textures. Alteration products include abundant sericite and clay minerals (Fig. 5c). Trace amounts of accessory fluorite are also observed in some samples.

The Aydos Formation is composed of quartz, K-feldspar, plagioclase, and opaque minerals. Quartz grains exhibit undulose extinction, interlocking edges, and elongated shapes. K-feldspar shows widespread alteration, whereas plagioclase occurs in minor amounts and displays zoning and polysynthetic twinning. Quartz overgrowths and outgrowth cements, formed under diagenetic to subsequent low-grade metamorphic conditions, highlight the orthoquartzite character of this formation (Fig. 5d).

Whole rock geochemistry

The whole-rock major and trace element compositions of the samples collected from the Lower Paleozoic clastic rocks of the Istanbul Zone are listed in Supplementary Table S1.

Geochemical classification of sandstones

Representative samples of the Ordovician–Silurian sediments from the Istanbul Zone were evaluated using the geochemical classification of Herron (1988). This approach, based on the log(SiO_2/Al_2O_3) and log(Fe_2O_3/K_2O) ratios, provides insights into both the lithological maturity of clastic rocks and the nature of their potential sources (Supplementary Table S2).

Samples from the Kocatöngel Formation plot entirely within the shale field (Fig. 6b). These values point to a compositionally immature character with a significant matrix content. Their distribution on the Fe_2O_3–MgO diagram (Fig. 6c) suggests deposition in marine–deltaic settings. Such features are consistent with detritus derived from nearby sources in tectonically active regions, most likely back-arc or magmatic arc environments (McLennan et al. 1993).

Samples from the Bakacak Formation (Ob1–Ob9) show log(SiO_2/Al_2O_3) values of 0.45–0.74 and log(Fe_2O_3/K_2O) values of 0.0–1.99, mostly plotting within the shale to Fe-shale

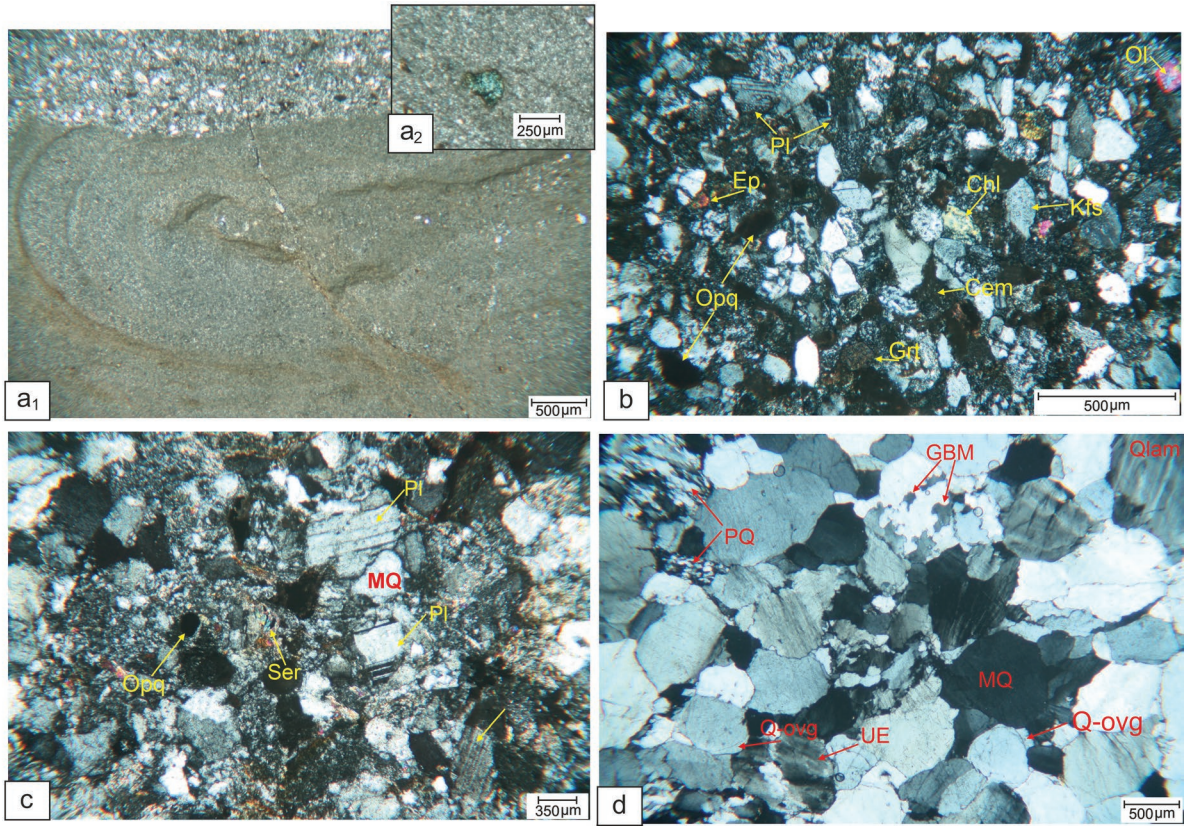


Fig. 5. Thin-section photomicrographs (crossed nicols) of Paleozoic clastic units from the Istanbul Zone: **a**$_1$ — Kocatöngel Formation, **a**$_2$ — Kocatöngel Formation with glauconite, **b** — Bakacak Formation, **c** — Kurtköy Formation, **d** — Aydos Formation. Abbreviations: Q=Quartz, Pl=Plagioclase, Ep=Epidote, Chl=Chlorite, Grt=Garnet, Opx/Opq=Opaque minerals, Ks=Calcite, O-m=Oligoclase, PQ=Polycrystalline quartz, MQ=Monocrystalline quartz, UE=Undulose extinction, GBM=Grain boundary migration, Q-ovg=Quartz overgrowth.

fields (Fig. 6b). Their clustering on the P_2O_5/TiO_2–MgO/CaO diagram (Fig. 6a) indicates a dominantly sedimentary signature characterized by low P–Ti ratios, consistent with enhanced sediment recycling and pre-depositional reworking (Werner 1987).

Samples from the Kurtköy Formation plot mainly within the shale and Fe-shale fields, with one sample extending into the Fe-sand field (Fig. 6b). Their positions on the Fe_2O_3–MgO diagram are fully consistent with all samples falling within the 'Non-marine and Deltaic Sandstone' field (Fig. 6c). When the XRD, CIA and ICV results are also considered together (Figs. 4, 7, 8), the samples collectively indicate pronounced chemical weathering, sedimentary reworking, and a relatively high degree of mineralogical maturity (McLennan et al. 1993).

In summary, the stratigraphic progression from fine-grained shale-dominated deposits of the Kocatöngel Formation to the feldspathic and ferruginous sandstones of the Bakacak and Kurtköy formations reflects an overall trend of increasing mineralogical and textural maturity. Although geochemical data are not available for the overlying Aydos Formation, XRD analyses indicate a quartz-dominated composition consistent with continued sedimentary reworking under relatively more stable conditions.

The major and trace element systematics of the Ordovician–Silurian clastics of the Istanbul Zone reveal clear geochemical fingerprints of provenance and tectonic setting. UCC-normalized major oxide patterns show depletion in CaO and Na_2O, together with enrichment in K_2O and Fe_2O_3, reflecting intense feldspar weathering and input from evolved felsic sources (Taylor & McLennan 1985; Nesbitt & Young 1989) (Supplementary Fig. S1). These features are consistent across the Kocatöngel, Bakacak, and Kurtköy formations, with the Bakacak and Kurtköy formations displaying higher K_2O contents related to K-feldspar and illite contributions.

UCC-normalized trace element patterns indicate pronounced negative Sr–Ba anomalies and enrichment in Th–Zr–Y, pointing to felsic-dominated sources with intermittent mafic contributions, especially in the Kurtköy Formation where Cr and Ni are elevated (Taylor & McLennan 1985; McLennan et al. 1990; Condie 1993) (Fig. 7a), and these patternsare consistent with the major and trace element characteristics of the North American Shale Composite (Gromet et al. 1984). Normalization values follow Rudnick & Gao (2014).

REE geochemistry provides additional constraints. The chondrite-normalized average REE patterns (Supplementary Fig. S2) of the Istanbul Zone clastics resemble PAAS,

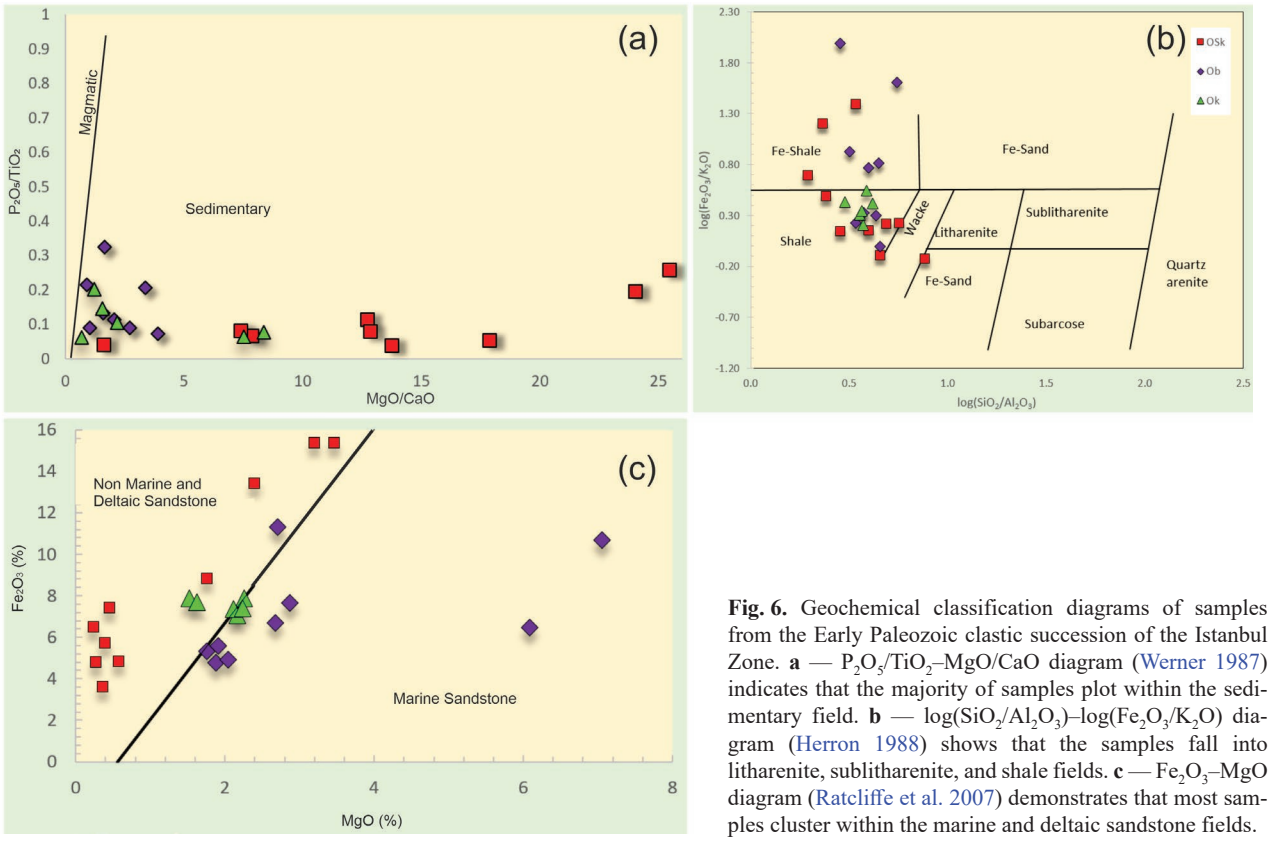
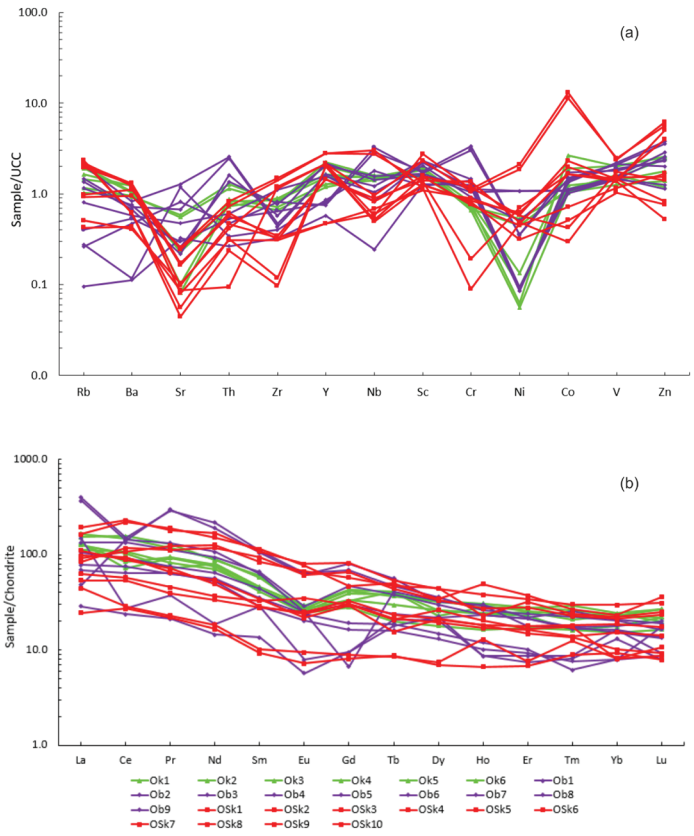


Fig. 6. Geochemical classification diagrams of samples from the Early Paleozoic clastic succession of the Istanbul Zone. **a** — P_2O_5/TiO_2–MgO/CaO diagram (Werner 1987) indicates that the majority of samples plot within the sedimentary field. **b** — $\log(SiO_2/Al_2O_3)$–$\log(Fe_2O_3/K_2O)$ diagram (Herron 1988) shows that the samples fall into litharenite, sublitharenite, and shale fields. **c** — Fe_2O_3–MgO diagram (Ratcliffe et al. 2007) demonstrates that most samples cluster within the marine and deltaic sandstone fields.



supporting an upper continental crust-dominated provenance (Taylor & McLennan 1985; McLennan 1989). Chondrite-normalized REE patterns of individual samples (Fig. 7b) show pronounced LREE enrichment, relatively flat HREE distributions, and marked negative Eu anomalies, indicating felsic provenance, feldspar fractionation, and recycling of upper continental crust (Taylor & McLennan 1985; McLennan 1989; McDonough & Sun 1995).

Paleoclimate, chemical weathering and redox indicators

The CIA–Al/Na diagram (Fig. 8c; Servaraj & Arthur 2006) highlights clear differences in the degree of weathering among the formations. Samples from the Kocatöngel Formation (Ok) plot in the moderately weathered zone with CIA values of ~65–72 and low Al/Na ratios (<50) (Fig. 8a, c). These values indicate limited chemical weathering in the source area, which is

Fig. 7. a — UCC-normalized multi-element variation (Rudnick & Gao 2014) and **b** — chondrite-normalized REE patterns (McDonough & Sun 1995) of all samples from the studied formations (Kocatöngel – green, Bakacak – purple, Kurtköy – red).

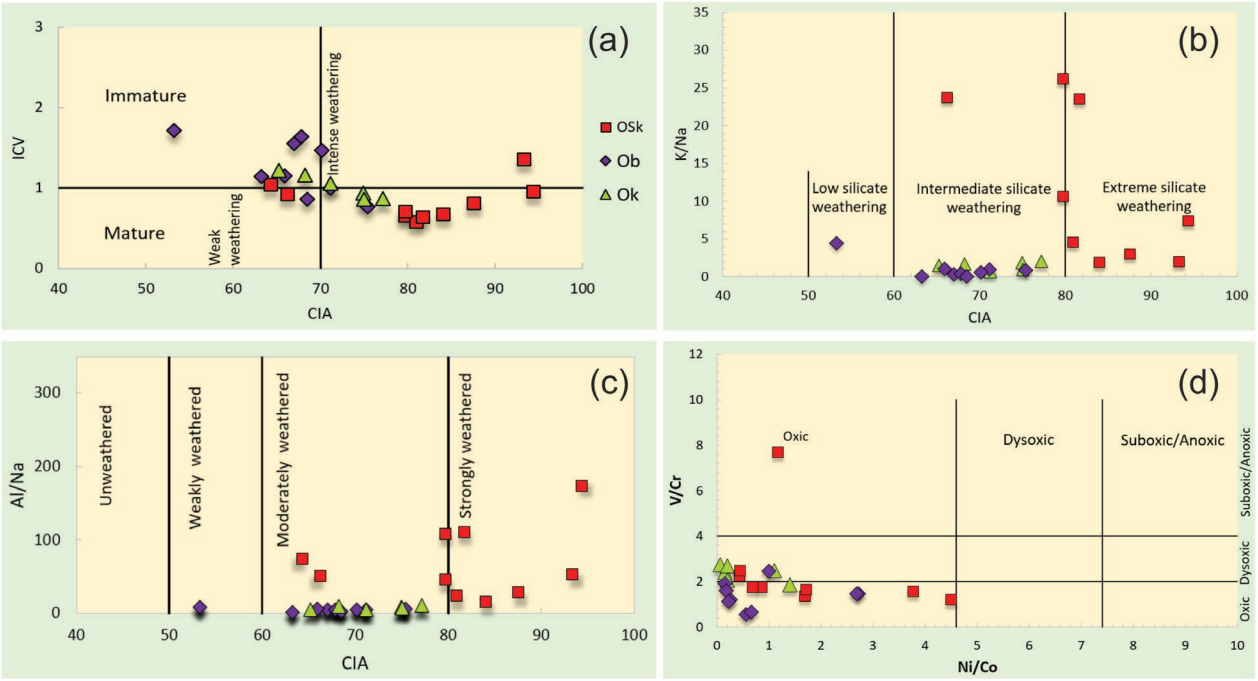


Fig. 8. Weathering indices and redox-sensitive element ratios for the Early Paleozoic clastic succession of the Istanbul Zone, including: **a** — ICV–CIA diagram (Nesbitt & Young 1982; Cox et al. 1995); **b** — K/Na–CIA diagram (Nesbitt & Young 1984; McLennan & Murray 1999); **c** — Al/Na–CIA diagram (Servaraj & Arthur 2006); **d** — V/Cr–Ni/Co ratios (Jones & Manning 1994; Tribovillard et al. 2006).

likely related to rapid burial processes that shortened the residence time of sediments at the surface, or to deposition under temperate climatic conditions (Nesbitt & Young 1982; Harnois 1988; Fedo et al. 1995). Samples from the Bakacak Formation (Ob) similarly display a moderately weathered character (Fig. 8a–c).

In contrast, samples from the Kurtköy Formation (OSk) yield CIA values of ~70–90 and mostly fall within the strongly weathered zone (Fig. 8a–c), implying prolonged exposure of the source region to intense chemical weathering.

For the Aydos Formation, XRD data and thin-section observations reveal quartz dominance and advanced feldspar alteration. The mineralogical composition and mature sandstone character indicate extensive chemical weathering and long transport in the source region. These features suggest deposition under tropical to subtropical climatic conditions.

The redox-sensitive element ratios (V/Cr and Ni/Co; Fig. 8d) indicate that most of the samples were deposited under oxic conditions, with only limited dysoxic–suboxic influences recorded at certain levels. These findings support the dominance of well-oxygenated shallow marine to terrestrial environments during deposition.

The observed differences among the formations reflect the combined influence of climatic conditions and source rock types on the weathering process and further suggest that stratigraphic variations in the degree of weathering may parallel the geodynamic evolution of the basin (Fig. 8a–d).

Provenance (source rock discrimination)

Source rock composition in the Early Paleozoic clastic succession of the Istanbul Zone was evaluated using major- and trace-element proxies (Fig. 9a–d). For this purpose, the major oxide–based SiO_2–Al_2O_3/TiO_2 diagram (Fig. 9a) and DF1–DF2 discriminant diagram (Fig. 9d) were combined with the trace element–based Th/Sc–Zr/Sc (Fig. 9b) and Co/Th–La/Sc (Fig. 9c$_1$) diagrams (Taylor & McLennan 1985; Roser & Korsch 1988; McLennan et al. 1993; Gu et al. 2002).

The SiO_2–Al_2O_3/TiO_2 relationship indicates felsic to quartzose dominance in the basal units of the succession, characterized by high SiO_2 contents and elevated Al_2O_3/TiO_2 ratios, whereas upward in the stratigraphy some subgroups show diversification with intermediate to mafic components (Fig. 9a; Roser & Korsch 1988; Hayashi et al. 1997). The DF1–DF2 diagram based on major oxides similarly confirms that most samples cluster within the Quartzose sedimentary and Felsic igneous fields, while a subset trends toward the Intermediate–Mafic igneous domain (Fig. 9d; Roser & Korsch 1988).

In the Th/Sc–Zr/Sc diagram, Th/Sc monitors the felsic–mafic proportion, whereas the Zr/Sc ratio tracks the heavy mineral/zircon concentration; when considered together, they allow the separation of source composition from grain-size or concentration effects (Fig. 9b; Taylor & McLennan 1985; McLennan et al. 1993). In the Co/Th–La/Sc diagram (logarithmic y-axis, linear x-axis), increasing Co/Th emphasizes mafic/basaltic input, while higher La/Sc highlights felsic

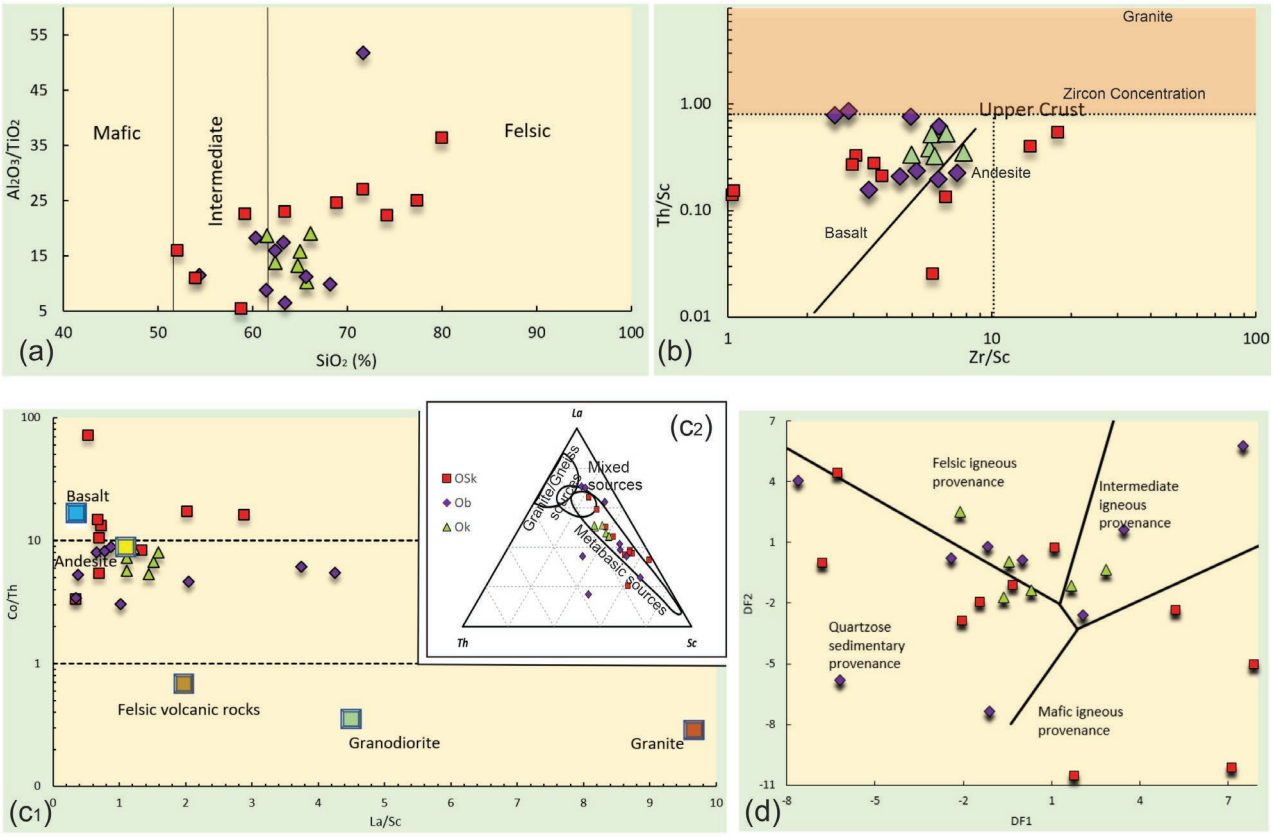


Fig. 9. Source-rock discrimination: **a** — SiO_2–Al_2O_3/TiO_2 (Al_2O_3/TiO_2 dimensionless) (Roser & Korsch 1988; Hayashi et al. 1997); **b** — Th/Sc–Zr/Sc (Taylor & McLennan 1985; McLennan et al. 1993); **c_1** — Co/Th–La/Sc (log y-axis, linear x-axis; fields for basalt–andesite, granite/granodiorite end-members) (Taylor & McLennan 1985; Cullers 2002; Gu et al. 2002); **c_2** — La–Th–Sc ternary diagram (inset) (Cullers 1994); **d** — DF1–DF2 discriminant function diagram with Quartzose sedimentary, Felsic igneous, Intermediate igneous, and Mafic igneous fields (Roser & Korsch 1988). Legend in panel (d): red squares=OSk, purple diamonds=Ob, green triangles=Ok.

contributions; the fields are read comparatively against basalt–andesite–granite/granodiorite end-members (Fig. 9c_1; Gu et al. 2002). The inset La–Th–Sc ternary plot (Fig. 9c_2) illustrates the expected mixing axis between felsic (La+Th enriched) and mafic (Sc enriched) poles using immobile ratios, thereby cross-validating the separation in panel Fig. 9c_1 (Bhatia & Crook 1986).

These source-rock proxies reveal a stratigraphic evolution from a predominantly felsic/quartzose base toward a more heterogeneous, multi-component provenance. The pattern is consistent with quartz-dominated textures and feldspathic components documented in the "Petrography" section; with the upward increase of deltaic–fluvial facies described in the "Stratigraphy and Sedimentology" section; and with zircon populations and temporal variations in zircon input shown in the "DZ U–Pb" section. The DF1–DF2 results based on major oxides independently corroborate the provenance interpretations derived from trace-element diagrams, confirming a felsic-dominated signature accompanied by limited to moderate mafic contributions (Taylor & McLennan 1985; Bhatia & Crook 1986; Roser & Korsch 1988; McLennan et al. 1993; Gu et al. 2002).

Tectonic setting indicators

Tectonic discrimination diagrams consistently indicate that the clastic succession was deposited in arc-related active margin settings (Figs. 10–12). In the DF1–DF2 plot of Bhatia (1983) (Fig. 10a), most samples fall within the OIA (Oceanic Island Arc) and ACM (Active Continental Margin) fields: Kocatöngel and Bakacak formation samples predominantly occupy the OIA domain, whereas many Kurtköy formation samples cluster within the ACM field, with only a few points extending toward the PM (Passive Margin) domain. This distribution reflects a predominantly volcanic-arc provenance, accompanied by an increasing continental influence in the younger parts of the succession. The Fe_2O_3+MgO–TiO_2 diagram (Fig. 10b) shows a comparable pattern, with most samples plotting along the oceanic-arc to continental-arc trend and no samples falling within the passive-margin field.

In all three ternary diagrams (Fig. 11a–c), the samples plot predominantly within the OIA field, with a secondary clustering in the CIA field and only a very limited number of points extending into the ACM field (Bhatia & Crook 1986). This consistent distribution across the diagrams indicates that the

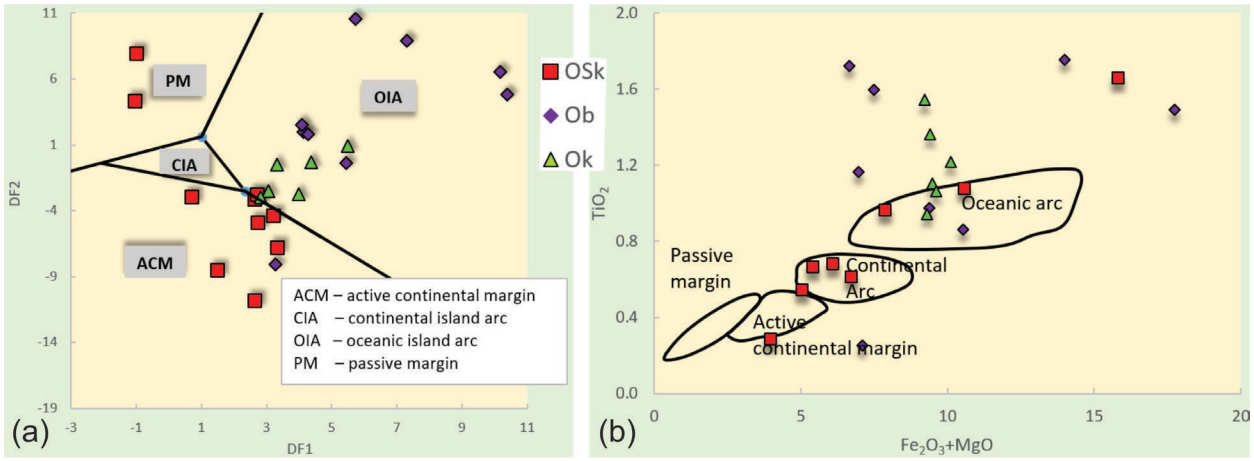


Fig. 10. Tectonic discrimination diagrams for the clastic rocks: **a** — DF1–DF2 (Bhatia 1983) – fields ACM, CIA, OIA, PM; **b** — Fe_2O_3+MgO* versus TiO_2 diagram (Bhatia 1983). Legend: red squares=OSk, purple diamonds=Ob, green triangles=Ok. Fe_2O_3 denotes total Fe expressed as Fe_2O_3.

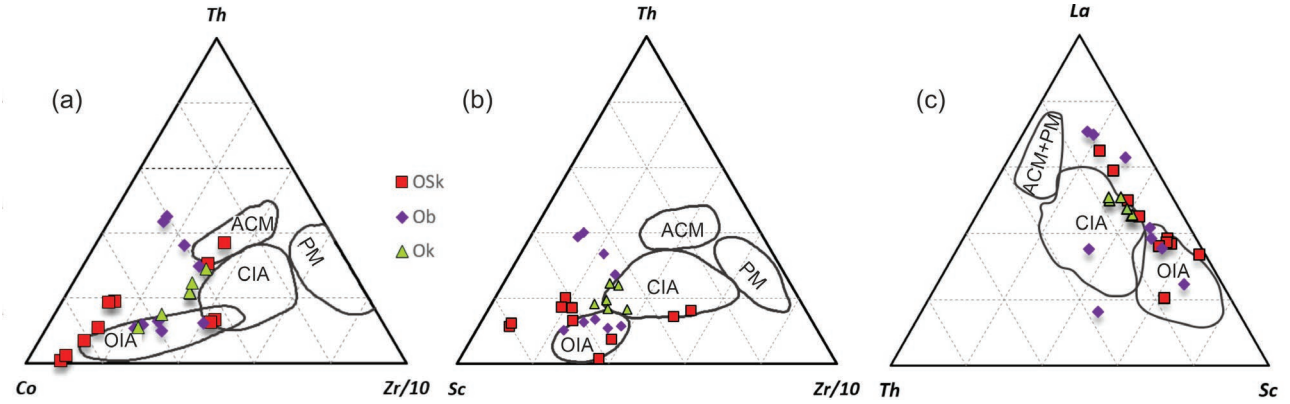


Fig. 11. Trace-element ternary discrimination diagrams for the tectonic setting of clastic rocks (Bhatia & Crook 1986). **a** — Th–Co–Zr/10; **b** — Th–Sc–Zr/10; **c** — La–Th–Sc. Fields: OIA – oceanic island arc, CIA – continental island arc, ACM – active continental margin, PM – passive margin.

detritus of the Early Paleozoic succession was largely supplied from oceanic island–arc sources, accompanied by subordinate input from continental island–arc settings and only a minor active-margin component. Such provenance patterns are characteristic of clastic systems developed along tectonically active plate margins where oceanic arc detritus dominates, yet limited material derived from adjacent continental arcs or continental margins is also incorporated.

Arc-affinity indicators (Fig. 12) further confirm this interpretation (Chakrabarti et al. 2007). Nb/Ta–Zr/Sm data (OSk, Ob, Ok) cluster predominantly within the IAB/Global Arc field, with some subgroups trending toward the MORB/OIB boundary (Fig. 12a). In the Ce–Ce/Pb diagram, low Ce/Pb values are consistent with Pb enrichment by subduction-related fluids (Fig. 12b) (Taylor & McLennan 1985; Hofmann et al. 1986). Because the Zr/Sm ratio may be sensitive to zircon concentration, the interpretation is supported by Ce/Pb as an independent indicator of subduction-related fluid enrichment

The subgroups plotting near the MORB/OIB boundary in Fig. 12, when considered together with the stratigraphic thickening of transgressive and marine facies described in the "Stratigraphy and Sedimentology" section, may suggest a partial contribution from back-arc extension or localized rifting processes. This implication aligns with models of rifting and the opening of the Paleo-Tethys along the northern margin of Gondwana (e.g., Nance et al. 2010; Stampfli et al. 2013).

U–Pb ages of detrital zircons

A total of 571 zircon analyses were performed, of which 513 yielded concordant $^{206}Pb/^{238}U$ ages (≈90 % of the dataset). Concordance was defined as a $^{206}Pb/^{238}U$–$^{207}Pb/^{235}U$ age agreement within 90–110 %. The concordant analyses were obtained from five representative samples (Ok: n=86, Ob1: n=99, Ob2: n=82, OSk1: n=129, OSk2: n=117) (Supplementary Table S4, Fig. 13). The remaining 58 discordant analyses (~10 %) were excluded from further interpretation.

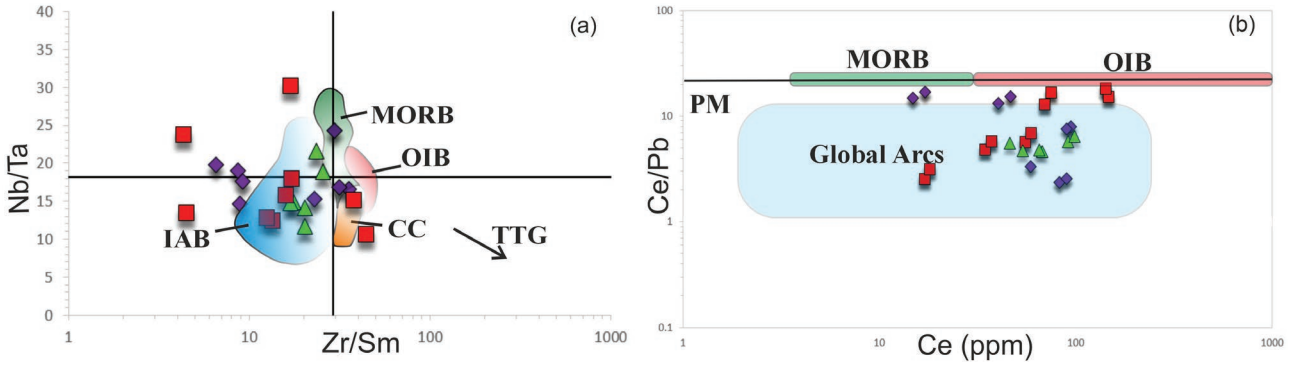


Fig. 12. Tectonic discrimination diagrams for the Early Paleozoic clastic succession of the Istanbul Zone: **a** — Nb/Ta versus Zr/Sm plot showing the tectonic affinity of the protolith; **b** — Ce versus Ce/Pb binary plot indicating the paleo-tectonic setting of the samples. IAB=Island Arc Basalts, CC=Continental Crust, OIB=Oceanic Island Basalts, MORB=Mid-Ocean Ridge Basalts; PM=Passive Margin (Chakrabarti et al. 2007; Kasanzu et al. 2017).

The Ok sample (basal part of the succession) yields youngest $^{206}Pb/^{238}U$ ages of ~480–490 Ma, (mean ≈484 Ma) constraining deposition to the Early Ordovician (Tremadoc–Floian). KDE plots (Fig. 14a) reveal a prominent peak at 540–560 Ma, consistent with the Pan-African orogenic cycle (Kröner & Stern 2004; Meert 2003; Bonev et al. 2025). An additional density of ages around 500–520 Ma is interpreted as reflecting detrital input derived from widespread post-Pan-African/Cadomian magmatic arcs active along the northern Gondwana margin, whose products were subsequently reworked into the basin prior to deposition (Meinhold et al. 2010).

The youngest concordant $^{206}Pb/^{238}U$ ages of ~460 Ma obtained from the Ob1 and Ob2 samples of the Bakacak Formation (Fig. 14b, c) indicate that deposition was not restricted to the Middle Ordovician, but also continued into the late Middle to Early Late Ordovician (Darriwilian–Sandbian), demonstrating that the uppermost part of the formation reached this interval. This interpretation is further constrained by the youngest concordant age of 460±22 Ma (YSG), which defines the maximum depositional age (MDA); a coherent cluster of two grains at 460–461 Ma (YC2σ, mean =460.5±14 Ma) provides additional support for a Middle to early Late Ordovician (Darriwilian–Sandbian) estimate. Considering both field observations and the stratigraphic continuity with the overlying Kurtköy Formation, it is evident that the transition into the Silurian occurred within a stratigraphically continuous succession. The KDE curves display a Pan-African peak at ~550–600 Ma, while the younger ~460–470 Ma peaks reflect syn-sedimentary magmatic inputs.

Considering both field observations and the stratigraphic continuity with the overlying Kurtköy Formation, it is evident that the transition into the Silurian occurred within a stratigraphically continuous succession. The Kurtköy Formation yields a youngest concordant $^{206}Pb/^{238}U$ age of 436±12 Ma (YSG) (Supplementary Table S4; Figs. 13 and 14d, e), demonstrating that deposition continued into the Early Silurian (Llandovery). A cluster of grains at 447–460 Ma (YC2σ) constrains the MDA to the latest Middle–early Late Ordovician (Darriwilian–Sandbian transition), while an additional group at 473–498 Ma reflects reworked Early Ordovician sources. The KDE curves preserve the Pan-African peak at ~540–560 Ma and, in addition, younger peaks at ~440–450 Ma prominently emerge, consistent with Silurian deposition (Fig. 14d–f).

The Cumulative Age Distribution (Fig. 15a) curves indicate that all samples share a similar provenance signal. The typical detrital zircon age proportions reported for peri-Gondwanan source regions – (1) Cadomian–Pan-African (500–600 Ma), (2) Grenvillian (~900–1200 Ma), (3) Mesoproterozoic (1300–1600 Ma), (4) Paleoproterozoic (~1.9–2.2 Ga), and A minor Neoarchean component (>2.5 Ga) – represent general regional averages documented in the literature (Stern 1994; Condie 1998; Abdelsalam et al. 2002; Meinhold et al. 2010; Johnson et al. 2011). This distribution is particularly distinct in the peri-Gondwanan terranes located in Europe, which were accreted to Laurussia during the Late Paleozoic; their sedimentary record reflects the structure of the source areas in the main Gondwanan continent – primarily the North African–Arabian Nucleus – that supplied these regions.

These age intervals are fully consistent with typical peri-Gondwanan provenance patterns; however, the distributions observed in this study show a particularly strong Cadomian–Pan-African dominance. The Cumulative Age Distribution (CAD) curves (Fig. 15a), based on 513 concordant zircon analyses, reveal three principal age groups that account for the vast majority of the detrital zircon population: (1) Post-Pan-African (436–500 Ma; 5.6 %), (2) Cadomian–Pan-African (500–600 Ma; dominant peak), and (3) Cryogenian (635–720 Ma; 11.3 %). In contrast, older Precambrian components occur only as minor populations – including Grenvillian (~900–1200 Ma), Mesoproterozoic (1300–1600 Ma), and Paleoproterozoic (~1.9–2.2 Ga), each representing approximately 1–2 % of the total zircon population – together with a very minor Neoarchean component (>2.5 Ga; <1 %). These age populations therefore reflect a provenance dominated by peri-Gondwanan crustal blocks, most notably the Arabian–Nubian Shield and the Saharan Metacraton, consistent with

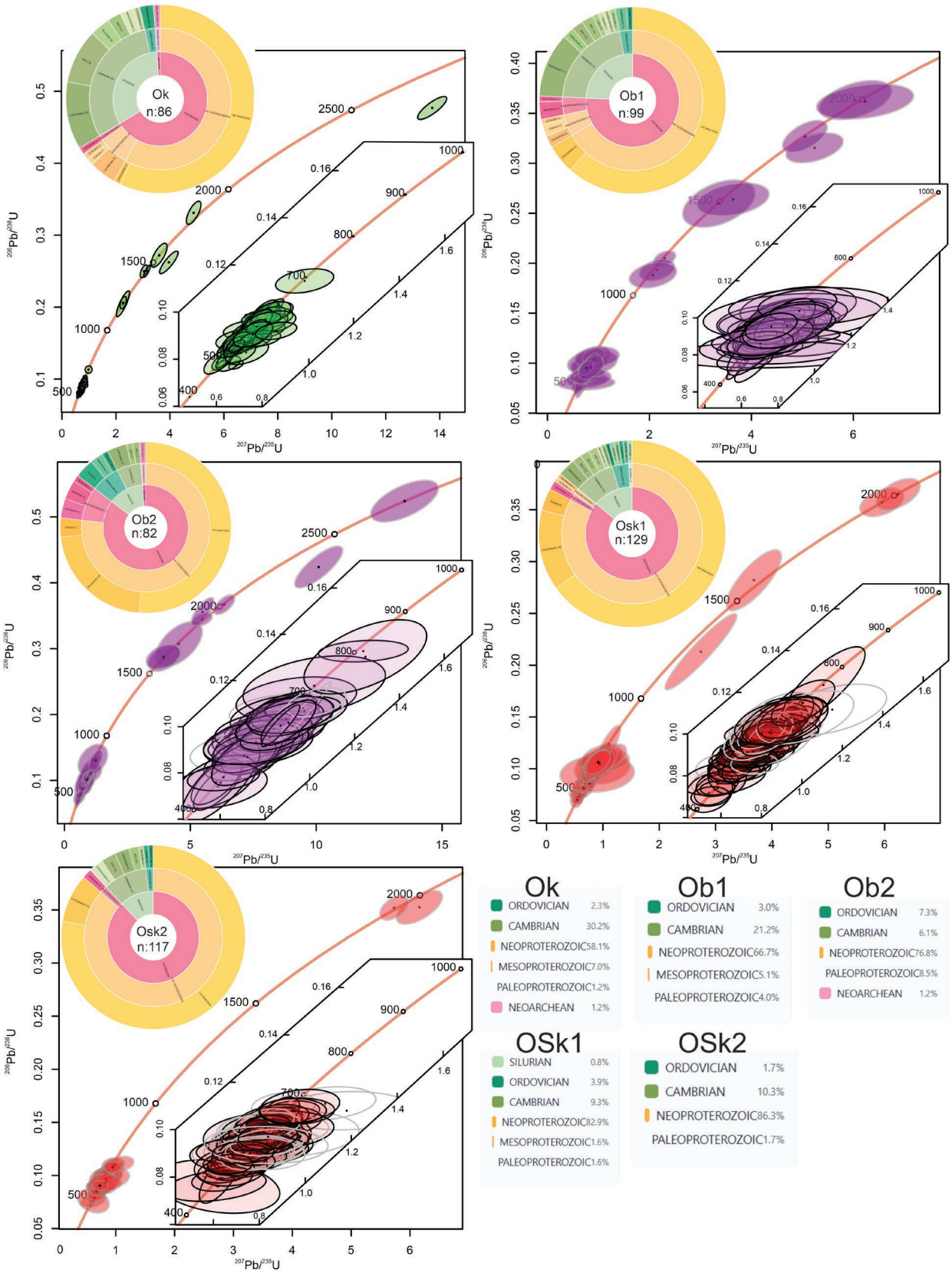


Fig. 13. Concordia diagrams of detrital zircon U–Pb results from representative samples of the Early Paleozoic clastic succession of the Istanbul Zone (Ok: Kocatöngel, Ob1–Ob2: Bakacak, OSk1–OSk2: Kurtköy formations). Each panel also includes age histograms and circular diagrams showing zircon age distributions by stratigraphic periods, with the corresponding percentage contributions summarized in the legend.

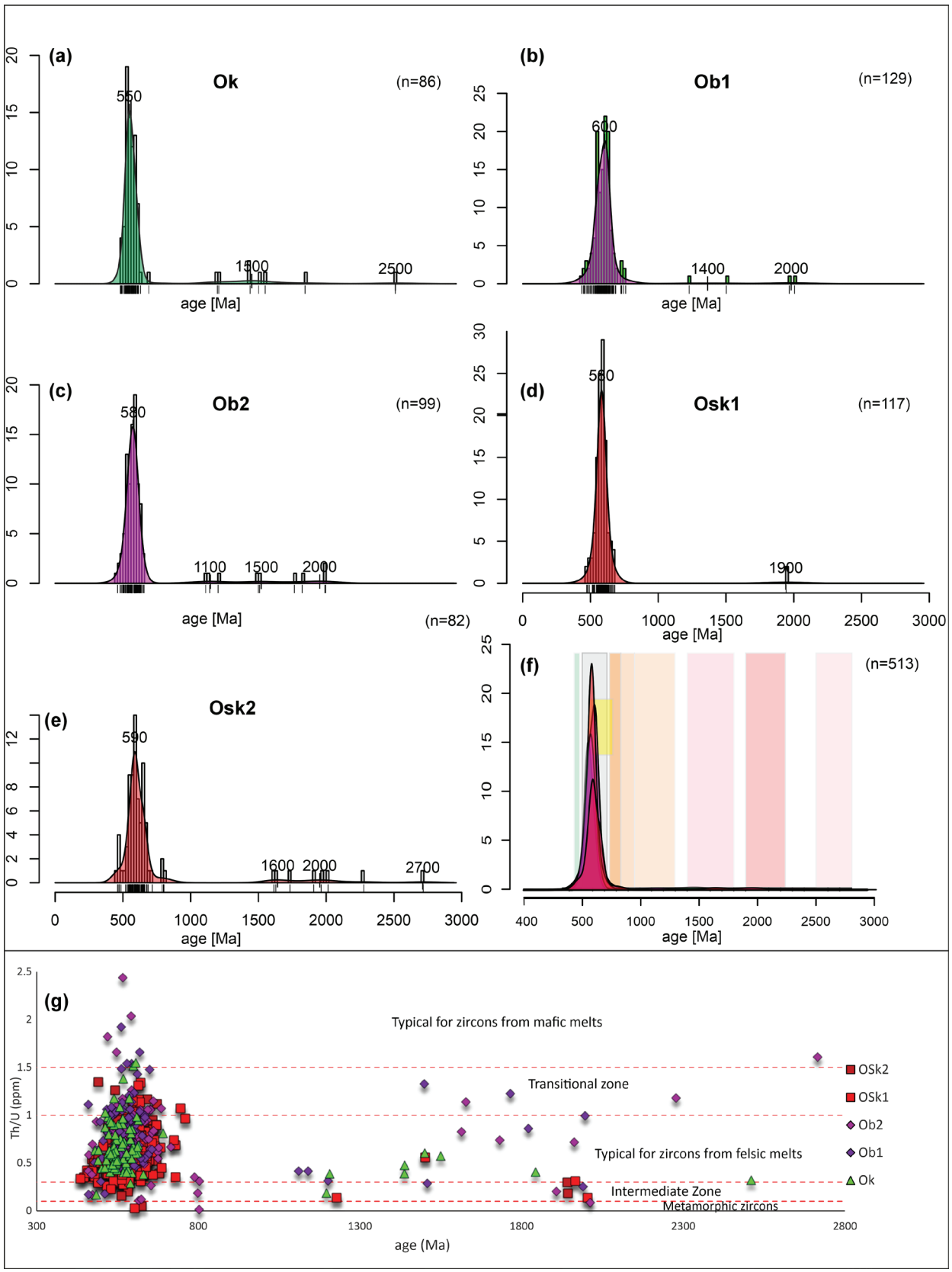


Fig. 14. a–f — Kernel density estimate (KDE) histograms of detrital zircon U–Pb ages from individual samples; the final panel shows all samples combined with shaded vertical bands marking major crustal growth and orogenic events (band colors as in Fig. 15). **g** — Th/U ratio versus age diagram distinguishing magmatic and metamorphic zircon populations. Reference fields and boundary values between zircon types are after Teipel et al. (2004) and Linnemann et al. (2011).

the paleogeographic position of the Istanbul Zone along the northern margin of Gondwana during the Ordovician–Silurian. The elevated proportion of Cryogenian zircons reflects early Neoproterozoic magmatic activity associated with rift or back-arc development behind the Cadomian arc. This interpretation is consistent with geodynamic models that document intra-arc and back-arc extension along the northern margin of Gondwana during Cadomian arc evolution (e.g., von Raumer et al. 2015; Bonev et al. 2025).To complement the U–Pb detrital zircon age interpretations, we additionally applied the tectonic discrimination method of Cawood et al. (2012). This approach evaluates the difference between zircon crystallization ages (CA, crystallization age) and the depositional age of the host unit (DA, depositional age), and plots these values (CA–DA) as cumulative proportion curves. Variations in the youngest 5–30 % of the population allow discrimination between convergent/active margin, collisional, and extensional/passive-margin settings. In this framework, low CA–DA values – particularly <100 Ma in the youngest 30 % and <150 Ma in the youngest 5 % – indicate syn- or near-synmagmatic input typical of active margins, whereas higher values reflect older basement sources characteristic of collisional or extensional regimes.

Applying this method to the Istanbul Zone samples (Ok, Ob1, Ob2, OSk1, OSk2) reveals that all cumulative curves fall distinctly within the active margin (A) field. Each sample exhibits a steep initial rise in the CA–DA curves, with more than 30 % of the zircon population yielding CA–DA values <100 Ma, and the youngest 5 % showing values well below the ≥150 Ma threshold that defines passive-margin settings. Although Ob2 displays a slightly broader spread, approaching the A–B transition, it still maintains a predominantly arc-derived signature. Overall, the CA–DA distributions strongly indicate that sedimentation occurred in proximity to an active magmatic arc, consistent with a convergent peri-Gondwanan margin rather than a stable cratonic or intraplate setting (Fig. 15b).

The Th/U–age diagram (Fig. 14g) shows that the majority of zircons are of magmatic origin (Th/U>0.3; 70–80 %). A smaller subgroup with low Th/U values (<0.1; 5–10 %) is of metamorphic character, occurring predominantly within the 600–700 Ma interval. This indicates that, in addition to magmatic arc–derived grains, recycled basement rocks also contributed to the basin.Detrital zircon KDE analyses were performed using a bandwidth of 30 Myr and a bin width of 20 Myr. Narrower bandwidths may generate artificial peaks, whereas broader ones may obscure true provenance signals (Vermeesch 2012; Spencer et al. 2016). Therefore, these parameters provide an optimum resolution that is widely accepted in detrital zircon provenance studies.

In summary, the $^{206}Pb/^{238}U$ ages constrain the maximum depositional age of the studied succession to the Early–Middle Ordovician (~480–460 Ma), while Silurian (~440–450 Ma) ages from the Kurtköy Formation indicate that sedimentation continued into the Early Silurian. The KDE and CAD data clearly demonstrate the dominant contributions from the Pan-African–Cadomian orogenic belts, together with minor Grenvillian and Paleoproterozoic components, highlighting the unequivocal peri-Gondwanan affinity of the basin.

Discussion

Stratigraphic onset of sedimentation in the Istanbul Zone

The basal levels of sedimentation overlying the metamorphic basement in the Istanbul Zone have been interpreted differently by previous studies. Ustaömer et al. (2011) defined the conglomerates of the Kurtköy Formation as the lowermost clastic unit, whereas Yılmazer et al. (2025) considered both the Kurtköy and Bakacak formations. In these studies, the youngest detrital zircon grains obtained from the Aydos Formation quartzites in different localities (Istanbul, Karadere) yielded ages of 530 Ma (Ustaömer et al. 2011) and 535 Ma (Yılmazer et al. 2025). In these studies, the obtained ages, together with the conformable overlying relationship of the quartzites on the underlying conglomeratic levels, were evaluated, and this unit was shown as Ordovician in age in the stratigraphic sections. Although the youngest zircon ages obtained from all three samples (530–552 Ma) are consistent with the uppermost Cambrian–lowermost Ordovician stratigraphic age of the litharenites, Yılmazer et al. (2025) calculated the maximum depositional ages using the weighted mean ages of the youngest coherent zircon clusters and consequently obtained older values ranging from 544 to 582 Ma. They also emphasized that the dominant late Ediacaran detrital zircon population (589–610 Ma; particularly the 601–608 Ma peak) reflects the signature of late Neoproterozoic continental-arc magmatism and records the timing of the oceanic arc–continent collision. Within this tectonic framework, they proposed that this collision was followed by post-collisional uplift and erosion throughout the Cambrian, and that the deposition of the litharenites in the Istanbul Zone most likely commenced between the latest Cambrian and earliest Ordovician. However, our field observations indicate that sedimentation in the basin did not begin with the Kurtköy or Bakacak formations. Instead, it started with a thick (up to 1800 m) succession of fine-grained, laminated marine clastics (the Kocatöngel Formation), which underlie the coarse clastics and are transitional and conformable with them. These greenish-grey, fine-grained deposits display variable thickness (decreasing eastward) and are widely exposed in Istanbul (Sancaktepe, Çavuşbaşı) and Sakarya (Çamdağ). Therefore, the discrepancy between our results and those of previous studies primarily arises from the stratigraphic level chosen to define the “young cover.”

The base of the ~3500-m-thick succession underlying the quartzites of the Aydos Formation is tectonically bounded in the study area. This clastic succession begins with subtidal marine levels and shallows upward into fluvial and deltaic environments, with its lowermost part represented by the Kocatöngel Formation. Zircon ages obtained from this formation indicate that sedimentation in the Istanbul Zone began in

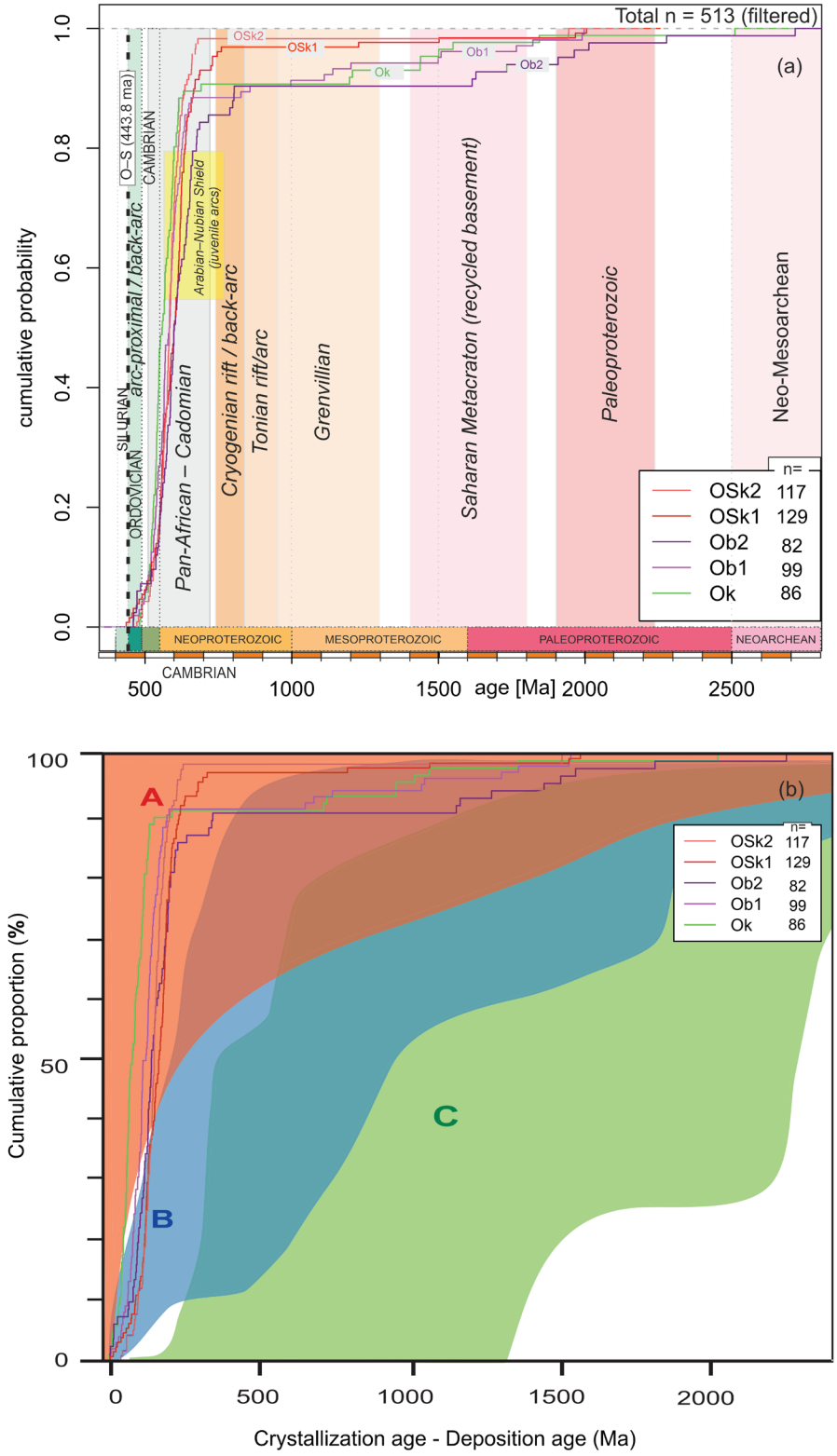


Fig. 15. a — Cumulative age distributions (CAD) for detrital zircons—Ok, Ob1, Ob2, OSk1, OSk2. The Ordovician–Silurian (O–S) boundary at 443.1 Ma is shown as a bold dashed line. Semi-transparent background bands denote potential source windows: Pan-African–Cadomian (650–520 Ma; emphasis at 550–600 Ma), Cryogenian rift/back-arc (720–650 Ma), Tonian rift/arc (900–720 Ma), Grenvillian (1300–950 Ma), Saharan Metacraton—recycled basement (1.8–1.4 Ga), Paleoproterozoic (2250–1900 Ma) and Neo-/Mesoarchean (2800–2500 Ma). The left-shift of OSk1–OSk2 relative to Ok/Ob records an Ordovician onset with up-section younging into the Silurian (Total n=513 after filtering). **b** — CA–DA cumulative proportion curves of the same samples, calculated following the approach of Cawood et al. (2012). Background colors represent the tectonic fields of Active margin (A), Collisional (B), and Passive/Extensional margin (C) settings.

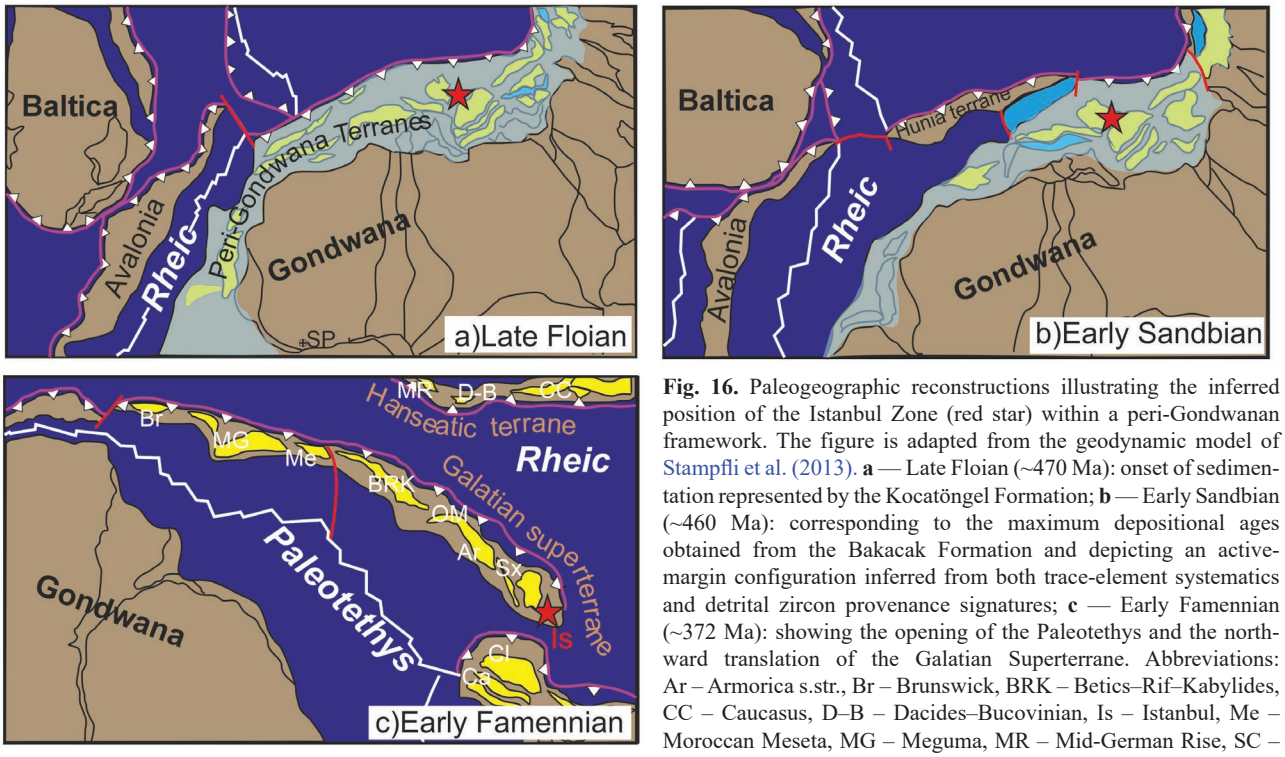


Fig. 16. Paleogeographic reconstructions illustrating the inferred position of the Istanbul Zone (red star) within a peri-Gondwanan framework. The figure is adapted from the geodynamic model of Stampfli et al. (2013). **a** — Late Floian (~470 Ma): onset of sedimentation represented by the Kocatöngel Formation; **b** — Early Sandbian (~460 Ma): corresponding to the maximum depositional ages obtained from the Bakacak Formation and depicting an active-margin configuration inferred from both trace-element systematics and detrital zircon provenance signatures; **c** — Early Famennian (~372 Ma): showing the opening of the Paleotethys and the northward translation of the Galatian Superterrane. Abbreviations: Ar – Armorica s.str., Br – Brunswick, BRK – Betics–Rif–Kabylides, CC – Caucasus, D–B – Dacides–Bucovinian, Is – Istanbul, Me – Moroccan Meseta, MG – Meguma, MR – Mid-German Rise, SC – South China, Sx – Saxothuringia.

the Early Ordovician.This regressive succession continued through the Upper Ordovician, when continental deposition became dominant, and persisted into the Early Silurian (Kurtköy Formation). Importantly, our findings also show that the Aydos quartzites, previously assigned an Ordovician age by earlier studies, should instead be regarded as a Wenlock-age transgressive unit. This interpretation is supported by their conformable and transitional relationship with the underlying Kurtköy Formation.

Source rock and tectonic setting interpretation

The detrital zircon U–Pb age spectra and geochemical data obtained in this study indicate that sedimentation in the Istanbul Zone predominantly developed within a continental arc setting influenced by upper-crustal sources. In particular, the decrease in Th/Sc ratios and the local enrichment in Zr/Sc ratios (Figs. 9, 10; Supplementary Table S3; Taylor & McLennan 1985; McLennan et al. 1993) suggest that sedimentation was mainly fed by felsic contributions, although limited mafic inputs were also present.

Tectonic discrimination diagrams based on whole-rock geochemistry (Figs. 11, 12; Bhatia & Crook 1986; Chakrabarti et al. 2007; Kasanzu et al. 2017) show that most samples cluster within the continental arc field, with only a few occupying intermediate positions. This implies that the Istanbul Zone succession was largely deposited under the influence of felsic continental crust, with subordinate contributions from mafic sources.

The zircon-based CAD diagram (Fig. 15a) further demonstrates that the age spectra are consistent with Pan-African and subordinate Grenvillian contributions characteristic of peri-Gondwanan terranes, reflecting direct ties with continental crustal sources (Nance & Linnemann 2008 and Linnemann et al. 2011). This supports the interpretation that the Istanbul Zone was supplied by continental basement terranes located along the northern margin of Gondwana.

Notable variations are also observed among the formations. The Kocatöngel and Bakacak formations reflect felsic to intermediate source regions of continental crustal affinity, characterized by moderate weathering and metamorphic input. In contrast, the Kurtköy Formation exhibits higher CIA values (Fig. 8; Nesbitt & Young 1982; Harnois 1988; Fedo et al. 1995) and clay enrichment, pointing to prolonged chemical weathering under increasingly humid conditions, accompanied by partial mafic contributions. At the top of the succession, the Aydos Formation is represented by mature quartz arenites, dominated exclusively by felsic, recycled crustal material.

These interpretations are strongly supported by isotopic evidence. Lu–Hf isotope analyses conducted on the sandstones of the Istanbul Zone by Yılmazer et al. (2025) revealed that the majority of Late Neoproterozoic zircons display negative initial εHf values (~78 %), whereas older Meso- and Paleoproterozoic zircons yield partially positive εHf signatures. This pattern indicates that Late Neoproterozoic magmatism was dominated by significant crustal involvement (~78 % negative εHf), whereas the older Meso- and Paleoproterozoic

zircon populations include a notable juvenile component as shown by their partially positive εHf signatures.

Taken together, both the geochemical discrimination diagrams (Figs. 9–12; Bhatia 1983; Taylor & McLennan 1985; Roser & Korsch 1986, 1988) and the zircon CAD results (Fig. 15a) clearly demonstrate the dominant role of continental crust in the Istanbul Zone, supplemented by minor mafic inputs. Isotopic data provide additional confirmation, highlighting the evolution of the Istanbul Zone within a continental arc system controlled primarily by crustal sources.

Neoproterozoic contributions (750–550 Ma)

Within the Neoproterozoic interval (750–550 Ma), zircon populations display two key components: a dominant Cadomian–Pan-African peak (500–600 Ma) and a subordinate yet significant Cryogenian group (~635–720 Ma). The pronounced zircon clusters between 750–550 Ma identified in the Istanbul Zone (Figs. 13, 14) are directly consistent with Pan-African/Cadomian orogenesis and play a key role in provenance interpretations. Ustaömer et al. (2011) linked zircons of this age group in the Istanbul Zone to Cadomian–Avalonian arc along the northern margin of Gondwana, while Chen et al. (2002) and Ustaömer et al. (2005) documented Pan-African granitoid intrusions within the Safranbolu and Bolu basement rocks, supporting this interpretation.

Although the late Neoproterozoic and Paleoproterozoic zircon populations further indicate a shared peri-Gondwanan heritage between the Istanbul and Strandja zones, detrital zircon and Lu–Hf data suggest that their sedimentary sources and paleogeographic positions diverged. At a later stage, however, the Lower Triassic clastics reveal a renewed connection and sediment supply from Upper Carboniferous–Lower Permian arc-related magmatic rocks of the Strandja Massif (Ülgen et al. 2018; Bonev et al. 2022).

von Raumer and Stampfli (2008) noted that, according to the literature, a maximum depositional age of approximately 600 Ma for the detrital sediments in the Alpine pre-Mesozoic basement is constrained by the youngest zircon grains (Schaltegger & Gebauer 1999; Thöni 1999). Such zircon assemblages have likewise been reported within the 'pre-orogenic age populations' of the Central Iberian domain (Martínez Catalán et al. 2004). Stephan et al. (2019) further classified peri-Gondwana detrital zircon records into four major provenance domains: Laurassian, Avalonian, West African, and East African–Arabian zircon provinces.

Our new zircon spectra (Fig. 14), together with the detrital zircon age distributions reported by Yılmazer et al. (2025) for Kurtköy and Aydos formations, demonstrate that both the eastern and western parts of the Istanbul Zone were supplied by Pan-African–aged basement sources. Consequently, the Neoproterozoic–Early Paleozoic age group represents the most robust shared signal, unequivocally confirming the attachment of the Istanbul Zone to the northern margin of Gondwana.

Mesoproterozoic contributions (1000–1600 Ma)

The limited zircon populations within the 1000–1600 Ma age range hold particular significance in discussions of the paleoprovenance of the Istanbul Zone. While zircons of this age are often attributed to Amazonian sources in classical Avalonian models, comparable contributions have also been documented in the Minoan domains of the central–eastern Mediterranean (Pelagonia, Attica–Cyclades, Crete, and the southern Aegean metamorphic complexes) (von Raumer & Stampfli 2008; Meinhold et al. 2010; Zlatkin et al. 2017). The zircon age spectra of the metasiliciclastics forming the Pelagonian basement are characterized by detrital populations in the 1.0–2.0 Ga range, with a prominent peak at around 1.5 Ga; this distribution has been linked to a peri-Amazonian affinity (Zlatkin et al. 2018). Consistent with this interpretation, the Mesoproterozoic signal documented in the Aydos quartzites by Ustaömer et al. (2011) (fig. 6 therein) indicates the view that the Istanbul terrane was located along the northwestern margin of Gondwana, in close proximity to Amazonia.

Nevertheless, the available data in the literature indicate that these age populations may have been derived from interior Gondwanan source regions as well as Amazonia. Pastore et al. (2023) reported that a minor Early Calymmian zircon cluster (~1576 Ma) occurs across both the Saharan dune fields and the Niger River tributaries, and noted that magmatism of this age is documented from the Leo Shield of the West African Craton to southeastern Nigeria. These data indicate that Early Calymmian magmatic belts within both the West African Craton and the Saharan Metacraton represent plausible sources of Mesoproterozoic detritus in peri-Gondwanan basins. This interpretation is further supported by evidence for extensive reworking of older crustal domains within the Saharan Metacraton (Abdelsalam et al. 2002).

Bonev et al. (2022) similarly emphasized that the Neoproterozoic–Cambrian zircons in the Sakar–Strandja Zone may have been derived from the Cadomian magmatic arc system, whereas the older Mesoproterozoic–Neoarchean zircons likely originated from the Sahara Metacraton and/or the Arabian–Nubian Shield in the interior of Gondwana. Taken together, these observations indicate that the 1000–1600 Ma Mesoproterozoic minor signal in the Istanbul Zone is best interpreted within a multiple-provenance framework that incorporates recycled crustal inputs from West Africa, the Saharan Metacraton, and Grenvillian terranes (Figs. 14, 15).

Paleoproterozoic contributions (1.8–2.2 Ga)

The limited zircon populations within the 1.8–2.2 Ga age range in the Istanbul Zone (Figs. 13–15; Supplementary Table S4) provide a critical signal of Gondwanan continental affinity. These ages reflect a pre-Pan-African continental basement and are directly comparable with the Paleoproterozoic cores of the West African Craton and the Saharan Metacraton (Abdelsalam et al. 2002).

Balintoni et al. (2011) identified Paleoproterozoic age peaks of 1.95–2.2 Ga from U–Pb dating of detrital zircons obtained from metasandstones and metaconglomerates of the late Neoproterozoic–early Cambrian Histria Formation within the Central Dobrogea terrane (Romania). They correlated these peaks with the characteristic 2.0–2.2 Ga age range of detrital zircons from the Amazon River, thereby suggesting a peri-Amazonian provenance for Central Dobrogea.

This evidence indicates that the Paleoproterozoic signal in the Istanbul Zone may reflect contributions from both African (West African Craton, Saharan Metacraton) and Amazonian sources. Moreover, as illustrated by Yılmazer et al. (2025, fig. 10c), similar Paleoproterozoic contributions are also documented in the Aydos Formation, suggesting that this signal is not a local anomaly yet a regionally persistent feature across the entire Istanbul Zone. Thus, Paleoproterozoic zircons represent a secondary but critical provenance indicator that strongly supports the Gondwanan affinity of the Istanbul Zone.

Archaean contributions (>2.5 Ga)

Three Neoarchean zircon grains (2.5–2.8 Ga) identified in the Istanbul Zone closely match the 2.7–2.5 Ga age interval characteristic of several Gondwanan cratons. This age range is widely documented in the basement rocks of the Saharan Metacraton (Abdelsalam et al. 2002), well established in the Reguibat Shield of the West African Craton (Key et al. 2008), and consistent with the Neoarchean–Early Paleoproterozoic granitoid assemblages known from the Congo Craton (Begg et al. 2009). Similar ages have also been reported from associated crustal blocks in Uganda and Tanzania (Johnson et al. 2003; Link et al. 2010). Therefore, these cratonic domains appear to be consistent with potential source regions for the rare Neoarchean zircons recorded in the Istanbul Zone. The presence of only a few Archean-aged zircons in the samples suggests that these grains, rather than representing an independent detrital source, may represent inherited zircon cores introduced into the system during the magmatic reworking of the underlying Archean crust.

Paleoclimate and weathering evolution

Mineralogical and geochemical variations across the succession provide a coherent record of progressive climatic change throughout the basin. In the Kocatöngel Formation, the presence of illite, muscovite, chlorite, vermiculite, and particularly glauconite (Figs. 4, 5), together with relatively low CIA values (~65–72) (Fig. 8a, c; Supplementary Table S2), points to deposition under cool semi-arid to temperate conditions characterized by rapid burial and limited chemical weathering. The Bakacak Formation reflects more energetic deltaic environments, exhibits moderate degrees of weathering (Fig. 8a–c) and significant metamorphic contributions (Fig. 5b).

Stratigraphically higher, the Kurtköy Formation displays elevated CIA values (~70–90) and enrichment in sericite/clay minerals (Fig. 5c; Fig. 8a–c), pointing to increasingly humid conditions and more intense chemical weathering. At the top of the succession, the Aydos Formation is represented by highly mature quartz-rich sandstones with feldspar depletion (Fig. 5d), which reflect advanced chemical weathering under tropical–humid climatic regimes.

These observations collectively align with global datasets documenting the shift from the Late Ordovician glacial conditions to greenhouse climate prevailing through the Silurian (Saltzman & Young 2005; Torsvik & Cocks 2017), and are consistent with previous paleoclimatic interpretations for the Istanbul Zone (Sayar & Cocks 2013). The temporal evolution of the mineralogical and chemical weathering indicators thus records a clear transition from cool semi-arid conditions at the base of the succession toward increasingly humid to tropical-humid climates upward, highlighting the strong influence of climatic regimes alongside source-rock variability and sediment transport processes in shaping the mineralogical composition of the basin.

Paleogeographic implications

Paleogeographically, the Istanbul Zone during the Ordovician developed along the northern margin of Gondwana (Fig. 16a, b), within a continental shelf-margin basin that initially formed under active continental margin conditions and subsequently evolved from cool semi-arid depositional environments to tropical–humid regimes during the Silurian. During its geodynamic evolution, the basin rifted away from Gondwana with the opening of the Paleo-Tethys Ocean and ultimately became positioned along the easternmost part of the Armorican domains within the Galatian superterrane (Figs. 1, 16c) (Stampfli & Borel 2002; Stampfli et al. 2013; von Raumer et al. 2013, 2015).

Importantly, our geochronological and geochemical results are not consistent with models that directly correlate the Istanbul Zone with NW Africa, Avalonia, or Amazonia, nor with scenarios proposing its detachment from Gondwana solely during the opening of the Rheic Ocean. Instead, the data reveal significant contributions from crustal sources linked to the Saharan Metacraton and Pan-African domains. They also record low-abundance yet geodynamically meaningful Grenvillian signals, supporting an evolutionary model in which the Istanbul Zone developed as a peri-Gondwanan continental margin basin progressively influenced by the opening of the Paleo-Tethys. This evolutionary trajectory ultimately culminated in the accretion of the Istanbul Zone to Laurussia during the Late Carboniferous Variscan orogeny.

Conclusions

- Detrital zircon ages obtained for the first time from the Kocatöngel Formation demonstrate that sedimentation in the Istanbul Zone initiated in the Early Ordovician.
- The Bakacak Formation was deposited during the Middle–Late Ordovician, while the Kurtköy Formation commenced

in the Late Ordovician and continued into the Early Silurian (Llandoverian). The overlying Aydos quartzites are interpreted as transgressive units.
- Geochemical data and zircon age spectra indicate that sedimentation was predominantly fed from felsic continental crustal sources, with only minor mafic input.
- Provenance signals reveal strong Pan-African/Cadomian (750–550 Ma) contributions, together with limited Mesoproterozoic, Paleoproterozoic, and rare Archaean zircons, all pointing to a Gondwanan affinity.
- Paleotectonically, sedimentation during the Ordovician developed in an active continental margin–arc setting, whereas during the transgressive period it continued under passive margin conditions.
- Paleogeographically, the Istanbul Zone represents a peri-Gondwanan continental margin basin that, with the opening of the Paleo-Tethys, became positioned along the eastern edge of the Armorican domains within the Galatian superterrane, and was finally accreted to Laurussia during the Variscan orogeny.

References

Abdelsalam M.G., Liegeois J.P. & Stern R.J. 2002: The Saharan Metacraton. *Journal of African Earth Sciences* 34, 119–136.

Akdoğan R., Hu X., Okay A.I., Topuz G. & Xue W. 2021: Provenance of the Paleozoic to Mesozoic siliciclastic rocks of the Istanbul Zone constrains the timing of the Rheic Ocean closure in the eastern Mediterranean region. *Tectonics* 40, e2021TC006824. https://doi.org/10.1029/2021TC006824

Amorosi A. 1997: Detecting compositional, spatial, and temporal attributes of glaucony: a tool for provenance research. *Sedimentary Geology* 109, 135–153. https://doi.org/10.1016/S0037-0738(96)00042-5

Arpat E., Tütüncü K., Uysal, S. & Göğer E. 1978: Safranbolu yöresinde Kambriyen- Devoniyen istifi. *TJK 32. Bilimsel ve Teknik Kurultayı, Bildiri Özetleri Kitabı,* 67–68 (in Turkish).

Aysal N., Şahin S.Y., Gungor Y., Peytcheva I. & Ongen S. 2018: Middle Permian–early Triassic magmatism in the Western Pontides, NW Turkey: Geodynamic significance for the evolution of the Paleo-Tethys. *Journal of Asian Earth Sciences* 164, 83–103. https://doi.org/10.1016/j.jseaes.2018.06.026

Bahlburg H. & Dobrzinski N. 2011: A review of the chemical index of alteration (CIA) and its application to the study of Neoproterozoic glacial deposits and climate transitions. The Geological Record of Neoproterozoic Glaciations. *Geological Society, London, Memoirs* 36, 81– 92. https://doi.org/10.1144/m36.6

Balintoni I., Balica C., Seghedi A. & Ducea M. 2011: Peri-Amazonian provenance of the Central Dobrogea terrane (Romania) attested by U/Pb detrital zircon age patterns. *Geologica Carpathica* 62, 299–307. https://doi.org/10.2478/v10096-011-0023-x

Begg G.C., Griffin WL., Natapov L.M., O'Reilly S.Y., Grand S.P., O'Neill C.J., Hronsky J., Poudjom Djomani Y., Deen T., Bowden P. & Aitken A.R. 2009: The lithospheric architecture of Africa: Seismic tomography, mantle petrology, and tectonic evolution. *Geosphere* 5, 23–50. https://doi.org/10.1130/GES00179.1

Bhatia M.R. 1983: Plate tectonics and geochemical composition of sandstones. *The Journal of Geology* 91, 611–627. https://doi.org/10.1086/628815

Bhatia M.R. & Crook K.A.W. 1986: Trace element characteristics of greywackes and tectonic setting discrimination of sedimentary basins. *Contributions to Mineralogy and Petrology* 92, 181–193. https://doi.org/10.1007/BF00375292

Black L.P. & Gulson B.L. 1978: The age of the Mud Tank carbonatite, Strangways Range, Northern Territory. *BMR Journal of Australian Geology & Geophysics* 3, 227–232. https://pid.geoscience.gov.au/dataset/ga/80964

Bonev N., Filipov P., Raicheva R. & Moritz R. 2022: Detrital zircon age constraints for Late Permian to Late Triassic clastic sedimentation in the northern-western Sakar-Strandzha Zone, SE Bulgaria. *International Journal of Earth Sciences* 111, 495–523. https://doi.org/10.1007/s00531-021-02125-6

Bonev N., Filipov P., Vladinova T., Stoylkova T., Georgieva H., Georgiev S., Kiselinov H. & Macheva L. 2025: U–Pb zircon age constraints on the Paleozoic sedimentation, magmatism and metamorphism of the Sredogriv metamorphics, Western Balkan Zone, NW Bulgaria. *Geosciences* 15, 1–18. https://doi.org/10.3390/geosciences15040148

Bozkaya Ö., Yalçın H. & Göncüoğlu M.C. 2002: Mineralogic and organic responses to the stratigraphic irregularities: An example from the Lower Paleozoic very low-grade metamorphic units of the Eastern Taurus Autochton, Turkey. *Schweizerische Mineralogische und Petrographische Mitteilungen* 82, 355–373. https://doi.org/10.5169/seals-62370

Bozkurt E., Winchester J.A., Yiğitbaş E. & Ottley C.J. 2008: Proterozoic ophiolites and mafic–ultramafic complexes marginal to the İstanbul Block: An exotic zone of Avalonian affinity in NW Turkey. *Tectonophysics,* 461, 240–251. https://doi.org/10.1016/j.tecto.2008.04.027

Boztug D. 1992: Lithostratigraphic units and tectonics of the southwestern part of Daday-Devrekani Massive, western Pontides, Turkey. *Bulletin of the Mineral Research & Exploration Institute of Turkey* 114, 1–22.

Castillo P., Bahlburg H., Fernandez R., Fanning C.M. & Berndt J. 2022: The European continental crust through detrital zircons from modernrivers: testing representativity of detrital zircon U–Pb geochronology. *Earth-Science Reviews* 232, 104145. https://doi.org/10.1016/j.earscirev.2022.104145

Cawood P.A., Hawkesworth C.J. & Dhuime B. 2012: Detrital zircon record and tectonic setting. *Geology* 40, 875–878. https://doi.org/10.1130/G32945.1

Chakrabarti R., Basu A.R. & Chakrabarti A. 2007: Trace element and Nd-isotopic evidence for sediment sources in the mid-Proterozoic Vindhyan Basin, central India. Precambrian Research 159, 260-274. https://doi.org/10.1016/j.precamres.2007.07.003

Chen F., Siebel W., Satır M., Terzioğlu M.N. & Saka K. 2002: Geochronology of the Karadere basement, NW Turkey and implications for the geological evolution of the Istanbul Zone. *International Journal of Earth Sciences* 91, 469–481. https://doi.org/10.1007/s00531-001-0239-6

Condie K.C. 1993: Chemical composition and evolution of the upper continental crust: Contrasting results from surface samples and shales. *Chemical Geology* 104, 1–37. https://doi.org/10.1016/0009-2541(93)90140-E

Condie K.C. 1998: Episodic continental growth and super-continents: A mantle avalanche connection? *Earth and Planetary Science Letters* 163, 97–108. https://doi.org/10.1016/S0012-821X(98)00178-2

Cox R., Lowe D.R. & Cullers R.L. 1995: The influence of sediment recycling and basement composition on evolution of mudrock chemistry in the southwestern United States. *Geochimica et Cosmochimica Acta* 59, 2919–2940. https://doi.org/10.1016/0016-7037(95)00185-9

Cullers R.L. 1994: The chemical signature of source rocks in size fractions of Holocene stream sediment derived from metamorphic rocks in the West Mountains region, USA. *Chemical Geology* 113, 327–343.

Cullers R.L. 2002: Implications of Elemental Concentrations for Provenance, Redox Conditions, and Metamorphic Studies of Shales and Limestones near Pueblo, Colorado, USA. *Chemical Geology* 191, 305–327.

Dean W.T., Martin F., Monod O., Demir O., Richards R.B., Bultynck P. & Bozdogan N. 1997: Lower Palaeozoic stratigraphy, Karadere-Zirze area, central Pontides, N Turkey. In: Göncüoğlu M.C. & Derman S. (Eds.): Early Palaeozoic Evolution in NW Gondwana. *Turkish Association of Petroleum Geologists Special Publications* 3, 32–38.

Dean W.T., Monod O., Rickards R.B., Demir O. & Bultynck P. 2000: Lower Palaeozoic stratigraphy and palaeontology, Karadere-Zirze area, Pontus Mountains, northern Turkey. *Geological Magazine* 137, 555–582. https://doi.org/10.1017/S0016756800004635

Dinis P., Garzanti E., Vermeesch P. & Huvi J. 2017: Climatic zonation and weathering control on sediment composition (Angola). *Chemical Geology* 467, 110–121. https://doi.org/10.1016/j.chemgeo.2017.07.030

Fedo C.M., Nesbitt H.W. & Young G.M. 1995: Unravelling the Effects of Potassium Metasomatism in Sedimentary Rocks and Paleosols, with Implications for Palaeo-Weathering Conditions and Provenance. *Geology* 23, 921–924. https://doi.org/10.1130/0091-7613(1995)023<0921:UTEOPM>2.3.CO;2

Gedik İ., Timur E., Duru M., Alan İ., Pehlivan Ş., Altun İ., Akbaş B., Önalan M. & Özcan İ. 2002: İstanbul Paleozoik istifinde Kocatöngel ve Bakacak formasyonları. *Türkiye Jeoloji Kurultayı Bildiriler Kitabı* 55, 97–99 (in Turkish).

Gehrels G. 2014: Detrital zircon U–Pb geochronology applied to tectonics. *Annual Review of Earth and Planetary Sciences* 42, 127–149. https://doi.org/10.1146/annurev-earth-050212-124012

Göncüoğlu M.C. 1997: Distribution of Lower Paleozoic rocks in the Alpine terranes of Turkey: Paleogeographic constraints. In: Göncüoğlu M.C. & Derman A.S. (Eds.): Lower Paleozoic Evolution in Northwest Gondwana. *Turkish Association of Petroleum Geologists Special Publications* 3, 13–24.

Göncüoğlu M.C. & Kozlu H. 2000: Early Paleozoic evolution of the NW Gondwanaland: Data from southern Turkey and surrounding regions. *Gondwana Research* 3, 315–324. https://doi.org/10.1016/S1342-937X(05)70290-2

Göncüoğlu M.C. & Kozur H. 1998: Facial development and alteration of Silurian rocks in Turkey In: Guiterrez Marco J.C. & Rabano I. (Eds.): Proceedings, 1998, Field Meeting. *IUGS Subcomission on Silurian Stratigraphy*, *Temas Gcolosico-Mineros ITGE*, Madrid, 23, 87–90.

Göncüoğlu M.C. & Kozur H. 1999: Differences in the geological evolution of the Istanbul and Zonguldak terranes, northern Turkey. In: Talent J.A., Khan F. & Mawson *R.* (Eds.): *Abstracts, IGCP 421 Peshawar Meeting, North Gondwanan mid-Palaeozoic bioevent/biogeography patterns in relation to crustal dynamics*. Peshawar, 16–18.

Göncüoğlu M.C., Turhan N., Şentürk K., Özcan A., Uysal Ş. & Yalınız M.K. 2000: A geotraverse across northwestern Turkey: Tectonic units of the Central Sakarya region and their tectonic evolution. *Geological Society, London, Special Publication* 173, 139–161. https://doi.org/10.1144/gsl.sp.2000.173.01.06

Görür N., Monod O., Okay A. I., Şengör A.M.C., Tüysüz O., Yiğitbaş E., Sakınç M. & Akkök R. 1997: Palaeogeographic and tectonic position of the Carboniferous rocks of the western Pontides (Turkey) in the frame of the Variscan belt. *Bulletin de la Société Géologique de France* 168, 197–205.

Gromet L.P., Haskin L.A., Korotev R.L. & Dymek R.F. 1984: The "North American shale composite": Its compilation, major and trace element characteristics. *Geochimica et cosmochimica acta* 48, 2469–2482.

Gu X.X., Liu J.M., Zheng M.H., Tang J.X. & Qi L. 2002: Provenance and Tectonic Setting of the Proterozoic Turbidites in Hunan, South China: Geochemical Evidence. *Journal of Sedimentary Research* 72, 393–407. https://doi.org/10.1306/081601720393

Haas W. 1968: Das Alt-Palaozoikum von Bithynien Nordwest-Türkei. *Neues Jahrbuch fur Geologie und Paläontologie Abhandlungen* 131, 178–242.

Harnois L. 1988: The CIW index: A new chemical index of weathering. Sedimentary *Geology* 55, 319–322. https://doi.org/10.1016/0037-0738(88)90137-6

Hayashi K., Fujisawa H., Holland H.D. & Ohmoto H. 1997: Geochemistry of 1.9 Ga sedimentary Rocks from Northeastern Labrador, Canada. *Geochimica et Cosmochimica Acta* 61, 4115–4137. https://doi.org/10.1016/S0016-7037(97)00214-7

Heineke C., Hetzel R., Nilius N.P., Zwingmann H., Todd A., Mulch A., Glotzbach C., Akal C.& Christl M. 2019: Detachment faulting in a bivergent core complex constrained by fault gouge dating and low-temperature thermochronology: The central Menderes Massif, western Turkey. *Journal of Structural Geology* 127, 103865. https://doi.org/10.1016/j.jsg.2019.103865

Herron M.M. 1988: Geochemical classification of terrigenous sands and shales from core or log data. *Journal of Sedimentary Research* 58, 820–829.

Hofmann A.W., Jochum K.P., Seufert M. & White W.M. 1986: Nb and Pb in oceanic basalts: new constraints on mantle evolution. Earth and Planetary Science Letters 79, 33–45.

Johnson P.R., Andresen A., Collins A.S., Fowler A.R., Fritz H., Ghebreab W., Kusky T. & Stern R.J. 2011: Late Cryogenian–Ediacaran history of the Arabian–Nubian Shield: A review of depositional, plutonic, structural, and tectonic events in the closing stages of the northern East African Orogen. *Journal of African Earth Sciences* 61, 167–232. https://doi.org/10.1016/j.jafrearsci.2011.07.003

Johnson S.P., Cutten H.N.C., Muhongo S. & De Waele B. 2003: Neoarchaean magmatism and metamorphism of the western granulites in the central domain of the Mozambique belt, Tanzania: U–Pb shrimp geochronology and PT estimates. *Tectonophysics* 375, 125–145. https://doi.org/10.1016/j.tecto.2003.06.003

Jones B. & Manning D.A.C. 1994: Comparison of geochemical indices used for the interpretation of palaeoredox conditions in ancient mudstones. *Chemical Geology* 111, 111–129. https://doi.org/10.1016/0009-2541(94)90085-X

Kasanzu C.H., Maboko M.A.H. & Manya S. 2017: Geochemistry and Sm-Nd systematics of the 1.67 Ga Buanji Group of southwestern Tanzania: Paleo-weathering, provenance and paleo-tectonic setting implications. *Geoscience Frontiers* 8, 1025–1037. https://doi.org/10.1016/j.gsf.2016.09.004

Kennedy A.K., Wotzlaw J.F., Schaltegger U., Crowley J.L. & Schmitz M. 2014: Eocene zircon reference material for microanalysis of U–Th–Pb isotopes and trace elements. *Canadian Mineralogist* 52, 409–421. https://doi.org/10.3749/canmin.52.3.409

Key R., Loughlin S., Gillespie M., Del Rio M.M., Horstwood M., Crowley Q.G., Darbyshire F., Pitfield P. & Henney P. 2008: Two Mesoarchaean terranes in the Reguibat Shield of NW Mauritania. In: Ennih N. & Liégeois J.-P. (Eds.): The Boundaries of the West African Craton. *Geological Society, London, Special Publication* 297, 33–52. https://doi.org/10.1144/SP297.3

Kröner A. & Stern R.J. 2004: Pan-African Orogeny. *Encyclopedia of Geology* 1, 1–12. https://doi.org/10.1016/B0-12-369396-9/00431-7

Link K., Koehn D., Barth M.G., Tiberindwa J.V., Barifaijo E., Aanyu K. & Foley S.F. 2010: Continuous cratonic crust between the Congo and Tanzania blocks in western Uganda. *International Journal of Earth Sciences* 99, 1559–1573. https://doi.org/10.1007/s00531-010-0548-8

Linnemann U., Ouzegane K., Drareni A., Hofmann M., Becker S., Gärtner A. & Sagawe A. 2011: Sands of West Gondwana: An archive of secular magmatism and plate interactions – A case study from the Cambro–Ordovician section of the Tassili Ouan Ahaggar (Algerian Sahara) using U–Pb-LA–ICP-MS detrital zircon ages. *Lithos* 123, 188–203. https://doi.org/10.1016/j.lithos.2011.01.010

Ludwig K.R. 2003: Mathematical–statistical treatment of data and errors for $^{238}U/^{206}Pb$ geochronology. *Reviews in Mineralogy and Geochemistry* 53, 631–656. https://doi.org/10.2113/0520631

Marroni M., Göncüoğlu M.C., Frassi C., Sayit K., Pandolfi L., Ellero A. & Ottria G. 2020: The Intra-Pontide ophiolites in Northern Turkey revisited: From birth to death of a Neotethyan oceanic domain. *Geoscience Frontiers* 11, 129–149. https://doi.org/10.1016/j.gsf.2019.05.010

Martínez Catalán J.R., Fernandez-Suarez J., Jenner G.A., Belousova E. & Diez Montes A. 2004: Provenance constraints from detrital zircon U–Pb ages in the Iberian Massif: implications for Palaeozoic plate configuration and Variscan evolution. *Journal of the Geological Society London* 161, 463–476. https://doi.org/10.1144/0016-764903-05

McCann T. 2008: The Geology of Central Europe. Volume 1: Precambrian and Palaeozoic; Volume 2: Mesozoic and Cenozoic. *Geological Society of London*. https://doi.org/10.1144/CEV1P

McDonough W.F. & Sun S.S. 1995: The composition of the Earth. *Chemical geology* 120, 223–253.

McLennan S.M. 1989: Rare earth elements in sedimentary rocks: influence of provenance and sedimentary processes. In: Lipin B.R. & McKay G.A. (Eds.): Geochemistry and Mineralogy of Rare Earth Elements. *Reviews in Mineralogy and Geochemistry* 21, 169–200. https://doi.org/10.1515/9781501509032-010

McLennan S.M. & Murray R.W. 1999: Geochemistry of sediments. In: Marshall C.P. & Fairbridge R.W. (Eds.): Encyclopedia of Geochemistry. *Kluwer Academic Publishers*, 282–292.

McLennan S.M., Taylor S.R., McCulloch M.T. & Maynard J.B. 1990: Geochemical and Nd–Sr isotopic composition of deep-sea turbidites: Crustal evolution and plate tectonic associations. *Geochimica et Cosmochimica Acta* 54, 2015–2050. https://doi.org/10.1016/0016-7037(90)90269-Q

McLennan S.M., Hemming S., McDaniel D.K. & Hanson G.N. 1993: Geochemical approaches to sedimentation, provenance, and tectonics. In: Johnsson M.J. & Basu A. (Eds.): Processes Controlling the Composition of Clastic Sediments. *Geological Society of America Special Paper* 285, 21–40. https://doi.org/10.1130/SPE284-p21

Meert J.G. 2003: A synopsis of events related to the assembly of eastern Gondwana. *Tectonophysics* 362, 1–40. https://doi.org/10.1016/S0040-1951(02)00629-7

Meinhold G., Kostopoulos D., Frei D., Himmerkus F. & Reischmann T. 2010: U–Pb LA-SF-ICP-MS zircon geochronology of the Serbo-Macedonian Massif, Greece: palaeotectonic constraints for Gondwana-derived terranes in the Eastern Mediterranean. *International Journal of Earth Sciences* 99, 813–832. https://doi.org/10.1007/s00531-009-0425-5

Moix P., Beccaletto L., Kozur H.W., Hochard C., Rosselet F. & Stampfli G.M. 2008: A new classification of the Turkish terranes and sutures and its implication for the paleotectonic history of the region. *Tectonophysics* 451, 7–39. https://doi.org/10.1016/j.tecto.2007.11.044

Nance R.D. & Linnemann U. 2008: The Rheic Ocean: origin, evolution, and significance. *GSA Today* 18, 4–12. https://doi.org/10.1130/GSATG24A.1

Nance R.D. & Murphy J.B. 1996: Basement isotopic signatures and Neoproterozoic paleogeography of Avalonian–Cadomian and related terranes in the circum-North Atlantic. In: Nance R.D. & Murphy J.B. (Eds.): Avalonian and related peri-Gondwanan terranes of the Circum-North Atlantic. *Geological Society of America* , 1–304. https://doi.org/10.1130/0-8137-2304-3.333

Nance R.D., Gutierrez-Alonso G., Keppie J.D., Linnemann U., Murphy J.B., Quesada C., Strachan R.A. & Woodcock N.H. 2010: Evolution of the Rheic Ocean. *Gondwana Research* 17, 194–222. https://doi.org/10.1016/j.gr.2009.08.001

Nesbitt H.W. & Young G.M. 1982: Early Proterozoic climates and plate motions inferred from major element chemistry of lutites. *Nature*, 299, 715–717. https://doi.org/10.1038/299715a0

Nesbitt H.W. & Young G.M. 1984: Prediction of some weathering trends of plutonic and volcanic rocks based on thermodynamic and kinetic considerations. *Geochimica et Cosmochimica Acta* 48, 1523–1534. https://doi.org/10.1016/0016-7037(84)90408-3

Nesbitt H.W. & Young G.M. 1989: Formation and diagenesis of weathering profiles. The *Journal of Geology* 97, 129–147. https://doi.org/10.1086/629290

Neubauer F. & Handler R. 2000: Variscan orogeny in the Eastern Alps and Bohemian Massif: How do these units correlate? *Austrian Journal of Earth Sciences* 92, 35–59.

Nikishin A.M., Okay A.I., Tüysüz O., Demirer A., Amelin D. & Petrov E. 2015: The Black Sea basins structure and history: New model based on new deep-penetration regional seismic data. Part 1: Basins structure and fill. *Marine and Petroleum Geology* 59, 638–655. https://doi.org/10.1016/j.marpetgeo.2014.08.017

Oberhänsli R., Candan O., Bousquet R., Rimmele G., Okay A. I. & Goff J. 2010: Alpine high pressure evolution of the eastern Bitlis complex, SE Turkey. In R. A. Stephenson et al. (Eds.), Sedimentary Basin Tectonics from the Black Sea and Caucasus to the Arabian Platform.*Geological Society, London, Special Publications* 340, 461–483. https://doi.org/10.1144/SP340.20

Oberhänsli R., Koralay E., Candan O., Pourteau A. & Bousquet R. 2013: Late Cretaceous eclogitic high-pressure relics in the Bitlis Massif (SE Turkey). *Geodinamica Acta* 26, 175–190. https://doi.org/10.1080/09853111.2013.858951

Odin G.S. & Matter A. 1981: De glauconiarum origine. *Sedimentology* 28, 611–641. https://doi.org/10.1111/j.1365-3091.1981.tb01925.x

Okay A.I. 1989: Tectonic units and sutures in the Pontides, northern Turkey. In: Şengör A.M.C. (Ed.): Tectonic Evolution of the Tethyan Region. *NATO Advanced ASI Series, Kluwer Academic Publications*, Dordrecht, 109–116.

Okay A.I. & Nikishin A.M. 2015: Tectonic evolution of the southern margin of Laurasia in the Black Sea region. *International Geology Review* 57, 1051–1076. https://doi.org/10.1080/00206814.2015.1010609

Okay A.I. & Topuz G. 2017: Variscan orogeny in the Black Sea region. *International Journal of Earth Sciences* 106, 569–592. https://doi.org/10.1007/s00531-016-1395-z

Okay A.I. & Tüysüz O. 1999: Tethyan sutures of northern Turkey. In: Durand B., Jolivet L., Horváth F. & ve Séranne M. (Eds.): The Mediterranean Basins: Tertiary extension within the Alpine orogen. *Geological Society, London, Special Publications* 156, 475–515. https://doi.org/10.1144/GSL.SP.1999.156.01.22

Okay A.I., Arman M.B. & Göncüoğlu M.C. 1985: Petrology and phase relations of the kyanite–eclogites from eastern Turkey. *Contributions to Mineralogy and Petrology* 91, 196–204. https://doi.org/10.1007/BF00377767

Okay A.I., Şengör A.M.C. & Görür N. 1994: Kinematic history of the opening of the Black Sea and its effect on the surrounding regions. *Geology* 22, 267–270. https://doi.org/10.1130/0091-7613(1994)022<0267:KHOTOO>2.3.CO;2

Okay A.I., Satır M., Maluski H., Siyako M., Monie P., Metzger R. & Akyüz S. 1996: Paleo- and Neo-Tethyan events in northwest Turkey: geological and geochronological constraints. In: Yin A. & Harrison M. (Eds.): Tectonics of Asia. *Cambridge University Press*, 420–441.

Okay A.I., Satır M. & Siebel W. 2006: Pre-Alpide orogenic events in the Eastern Mediterranean region. European Lithosphere Dynamics. *Geological Society, London, Memoirs* 32, 389–405. https://doi.org/10.1144/GSL.MEM.2006.032.01.23

Okay A.I., Bozkurt E., Satır M., Yiğitbaş E., Crowley Q.G. & Shang C.K. 2008: Defining the southern margin of Avalonia in the Pontides: geochronological data from the Late Proterozoic and Ordovician granitoids from NW Turkey. *Tectonophysics* 461, 252–264. https://doi.org/10.1016/j.tecto.2008.02.004

Okay A.I. Altıner, D., Sunal G., Tüysüz O., Aygül M., Akdoğan R., Altıner S. & Simmons M. 2018: Geological Evolution of the Central Pontides. In: Simmons M.D., Tari G.C. & Okay A.I. (Eds.): Petroleum Geology of the Black Sea. *Geological Society, London, Special Publications* 464, 33–67. https://doi.org/10.1144/SP464.3

Öksüm E., Hisarlı Z.M., Çinku M., Ustaömer T. & Orbay N. 2015: New paleomagnetic results from Ordovician sedimentary rocks from NW Anatolia; tectonic implications for the paleolatitudinal position of the Istanbul Terrane. *Tectonophysics* 664, 14–30. https://doi.org/10.1016/j.tecto.2015.08.014

Önalan M. 1981: Pendik bölgesi ile Adalar'ın jeolojisi ve sedimanter özellikleri. *İÜ Yerbilimleri Fak., Doç. tezi*, İstanbul, 1–193.

Özgül N. 2012: Stratigraphy and some structural features of the İstanbul Palaeozoic. *Turkish Journal of Earth Sciences* 21, 817–866. https://doi.org/10.3906/yer-1111-6

Paeckelmann W. 1938: Neue Beitrage zur Kenntnis des Geologie, Palaontologie und Petrographie der Umgegend von Konstantinople 2. Geologie Thraziens, Bithyniens und der Prinzeninseln. *Abhandlungen Preussischen Geologischen Landesanstalt* N.F. 168, 1–202.

Pastore G., Garzanti E., Vermeesch P., Bayon G., Resentini A., Braquet N. & Overare B. 2023: The zircon story of The Niger River: Time-structure maps of the West African Craton and discontinuous propagation of provenance signals across a disconnected sediment-routing system. *Journal of Geophysical Research: Earth Surface* 128. https://doi.org/10.1029/2023JF007342

Paton C., Hellstrom J., Paul B., Woodhead J. & Hergt J. 2011: Iolite: Freeware for the visualisation and processing of mass spectrometric data. *Journal of Analytical Atomic Spectrometry* 26, 2508–2518. https://doi.org/10.1039/C1JA10172B

Ratcliffe K.T., Morton A.C., Ritcey D.H. & Evenchick C.A. 2007: Whole-rock geochemistry and heavy mineral analysis as petroleum exploration tools in the Bowser and Sustut basins, British Columbia, Canada. Bulletin of Canadian Petroleum Geology 55, 320–336. https://doi.org/10.2113/gscpgbull.55.4.320

Roser B.P. & Korsch R.J. 1986: Determination of tectonic setting of sandstone–mudstone suites using SiO_2 content and K_2O/Na_2O ratio. *The Journal of Geology* 94, 635–650. https://doi.org/10.1086/629071

Roser B.P. & Korsch R.J. 1988: Provenance Signature of Sandstone-Mudstone Suites Determined Using Discriminant Function Analysis of Major Element Data. *Chemical Geology* 67, 119–139. https://doi.org/10.1016/0009-2541(88)90010-1

Rudnick R.L. & Gao S. 2003: The Composition of the Continental Crust. In: Holland H.D. & Turekian K.K. (Eds.): Treatise on Geochemistry. *Elsevier*, Oxford, 3, 1–64. https://doi.org/10.1016/B0-08-043751-6/03016-4

Rudnick R.L. & Gao S. 2014: Composition of the continental crust. In: Holland H. & Turekian K.K. (Eds.): Treatise on geochemistry, 2nd ed. *Elsevier*, Oxford, 4, 1–51. https://doi.org/10.1016/B978-0-08-095975-7.00301-6

Sachanski V., Göncüoğlu M.C., Lakova I., Boncheva I. & Demiray G. S. 2012: Silurian graptolite, conodont and cryptospore biostratigraphy of the Gülüç section in Ereğli, Zonguldak Terrane, NW Anatolia, Turkey. *Turkish Journal of Earth Sciences* 21, 867–903. https://doi.org/10.3906/yer-1004-4

Saltzman M.R. & Young S. 2005: Long-lived glaciation in the Late Ordovician? Isotopic and sequence-stratigraphic evidence from western Laurentia. *Geology* 33, 109–112. https://doi.org/10.1130/G21219.1

Sayar C. 1964: Ordovician Conularids from the Bosphorus Area, Turkey. *Geological Magazine* 101, 193–197. https://doi.org/10.1017/S0016756800049438

Sayar C. & Cocks L.R.M. 2013: A new Late Ordovician hirnantia brachiopod fauna from NW Turkey, its biostratigraphical relationships and paleogeographical setting. *Geological Magazine* 150, 479–496. https://doi.org/10.1017/S0016756812000520

Schaltegger U. & Gebauer D. 1999: Pre-Alpine geochronology of the central, western and southern Alps. *Schweizerische mineralogische und petrographische Mitteilungen* 79, 79–87.

Şen F. 2023: Ordovician arc and syncollisional magmatism in the İstanbul-Zonguldak Tectonic Unit (NW Turkey): Implications for the consumption of the Teisseyre-Tornquist Ocean in Far East Avalonia. *Mineralogy and Petrology* 117, 639–661. https://doi.org/10.1007/s00710-023-00812-7

Şengör A.M.C. & Yılmaz Y. 1981: Tethyan evolulution of Turkey: a plate tectonic approach. *Tectonophysics* 75, 181–241. https://doi.org/10.1016/0040-1951(81)90275-4

Servaraj K. & Arthur C.C. 2006: Moderate chemical weathering of subtropical Taiwan: constraints from solid-phase geochemistry ofsediments and sedimentary rocks. *Journal of Geology* 114, 101–116. https://doi.org/10.1086/498102

Sharkov E.V., Lebedev V.A., Rodnikov A.G., Chugaev A.V., Sergeeva N.A & Zabarinskaya L.P. 2012: Features of Caucasian segment of the Alpine-Himalayan convergence zone: geological, volcanological, neotectonical, and geophysical data. In: Sharkov E.V. (Ed.): Tectonic-Recent Advances. *InTech*, Rijeka, 37–52. https://doi.org/10.5772/50253

Spencer C.J., Kirkland C.L. & Taylor R.J. 2016: Strategies towards statistically robust interpretations of in situ U–Pb zircon geochronology. *Geoscience Frontiers* 7, 581–589.

Stampfli G.M. & Borel G.D. 2002: A plate tectonic model for the Paleozoic and Mesozoic constrained by dynamic plate boundaries and restored synthetic oceanic isochrons. *Earth and Planetary Science Letters* 196, 17–33. https://doi.org/10.1016/S0012-821X(01)00588-X

Stampfli G.M., Hochard C., Vérard C., Wilhem C. & von Raume J.F. 2013: The formation of Pangea. *Tectonophysics* 593, 1–19. https://doi.org/10.1016/j.tecto.2013.02.037

Stephan T., Kroner U. & Romer R.L. 2019: The pre-orogenic detrital zircon record of the Peri-Gondwanan crust. *Geological Magazine* 156, 281–307. https://doi.org/10.1017/S0016756818000031

Stern R.J. 1994: Arc assembly and continental collision in the Neoproterozoic East African Orogen: Implications for the consolidation of Gondwanaland. *Annual Review of Earth and Planetary Sciences* 22, 319–351. https://doi.org/10.1146/annurev.ea.22.050194.001535

Taylor S.R. & McLennan S.M. 1985: The Continental Crust: Its Composition and Evolution. *Blackwell Scientific*, Oxford, 1–312.

Teipel U., Eichhorn R., Loth G., Rohrmüller J., Höll R. & Kennedy A. 2004: U–Pb SHRIMP and Nd isotopic data from the western Bohemian Massif (Bayerischer Wald, Germany): Implications for Upper Vendian and Lower Ordovician magmatism. *International Journal of Earth Sciences* 93, 782–801. https://doi.org/10.1007/s00531-004-0419-2

Thöni M. 1999: A review of geochronological data from the Eastern Alps. *Schweizerische Mineralogische und Petrographische Mitteilungen* 79, 209–230.

Topuz G., Altherr R., Satır M. & Schwarz W.H. 2004: Low-grade metamorphic rocks from the Pulur Complex, NE Turkey: Implications for the pre-Liassic evolution of the Eastern Pontides. *International Journal of Earth Sciences* 93, 72–91. https://doi.org/10.1007/s00531-003-0372-5

Torsvik T.H. & Cocks L.R.M. 2013: Gondwana from top to base in space and time. *Gondwana Research* 24, 999–1030. https://doi.org/10.1016/j.gr.2013.06.012

Torsvik T.H. & Cocks L.R.M. 2017: Earth History and Palaeogeography. *Cambridge University Press*, 1–324.

Tribovillard N., Algeo T.J., Lyons T.W. & Riboulleau A. 2006: Trace metals as paleoredox and paleoproductivity proxies: An update. *Chemical Geology* 232, 12–32. https://doi.org/10.1016/j.chemgeo.2006.02.012

Ülgen S.C., Lom N., Sunal G., Gerdes A. & Sengor A.C.M. 2018: The Strandja Massif and the Istanbul zone were once part of the same tectonic unit: new data from Triassic detrital zircons. *Geodinamica Acta* 30, 212–224. https://doi.org/10.1080/09853111.2018.1475447

Ustaömer P.A., Mundil R. & Renne P.R. 2005: U/Pb and Pb/Pb zircon ages for arc-related intrusions of the Bolu Massif (W Pontides, NW Turkey): Evidence for Late Precambrian (Cadomian) age. *Terra Nova* 17, 215–223. https://doi.org/10.1111/j.1365-3121.2005.00594.x

Ustaömer P.A., Ustaömer T., Gerdes A. & Zulauf G. 2011: Detrital zircon ages from a Lower Ordovician quartzite of the İstanbul exotic terrane (NW Turkey): Evidence for Amazonian affinity. *International Journal of Earth Sciences* 100, 23–41. https://doi.org/10.1007/s00531-009-0498-1

van Hinsbergen D.J.J. 2010: A key extensional metamorphic complex reviewed and restored: The Menderes Massif of western Turkey. *Earth-Science Reviews* 102, 60–76. https://doi.org/10.1016/j.earscirev.2010.05.005

van Hinsbergen D.J.J., Dekkers M.J. Bozkurt E. & Koopman M. 2010: Exhumation with a twist: Paleomagnetic constraints on the evolution of the Menderes metamorphic core complex. *Tectonics* 29, TC3010. https://doi.org/10.1029/2009TC002596

Vermeesch P. 2012: On the visualisation of detrital age distributions. *Chemical Geology* 312–313, 190–194. https://doi.org/10.1016/j.chemgeo.2012.04.021

von Raumer J.F. & Stampfli G.M. 2008: The birth of the Rheic Ocean-Early Palaeozoic subsidence patterns and subsequent tectonic plate scenarios. *Tectonophysics* 461, 9–20. https://doi.org/10.1016/j.tecto.2008.04.012

von Raumer J.F., Bussy F., Schaltegger U., Schulz B. & Stampfli G. M. 2013: Pre-Mesozoic Alpine basements – their place in the European Paleozoic framework. *Geological Society of America Bulletin* 125, 89–108. https://doi.org/10.1130/B30654.1

von Raumer J.F., Stampfli G.M., Arenas R. & Sánchez Martínez S. 2015: Ediacaran to Cambrian oceanic rocks of the Gondwana margin and their tectonic interpretation. *International Journal of Earth Sciences* 104, 1107–112. https://doi.org/10.1007/s00531-015-1142-x

Werner C.D. 1987: Saxonian granulites – a contribution to the geochemical diagnosis of original rocks in high metamorphic complexes. *Gerlands Beiträge zur Geophysik* 96, 271–290.

Whitney D.L. & Bozkurt E. 2002: Metamorphic history of the southern Menderes massif, Western Turkey. *Geological Society of America Bulletin* 114, 829–838. https://doi.org/10.1130/0016-7606(2002)114%3C0829:MHOTSM%3E2.0.CO;2

Wiedenbeck M., Hanchar J.M., Peck W.H., Sylvester P., Valley J. et al. 2004: Further characterisation of the 91500 zircon crystal. *Geostandards and Geoanalytical Research* 28, 9–39. https://doi.org/10.1111/j.1751-908X.2004.tb01041.x

Yalçın M.N. & Yılmaz İ. 2010: Devonian in Turkey – a review. *Geologica Carpathica* 61, 235–253. https://doi.org/10.2478/v10096-010-0014-3

Yanev S., Göncüoğlu M.C., Gedik İ., Lakova I., Boncheva I., Sachanski V., Okuyucu C., Özgül N., Timur E., Maliakov Y. & Saydam G. 2006: Stratigraphy, correlations and palaeogeography of Palaeozoic terranes of Bulgaria and NW Turkey: a review of recent data. In: Robertson A.H.F. & Mountrakis D. (Eds.): Tectonic Development of the Eastern Mediterranean Region. *Geological Society, London, Special Publications* 260, 51–67. https://doi.org/10.1144/GSL.SP.2006.260.01.04

Yılmaz İ. 1977: Sancaktepe Granitinin (Kocaeli Yarımadası), mutlak yaşı ve jenezi: *Türkiye Jeoloji Bülteni* 20, 17–20 (in Turkish).

Yılmazer S., Topuz G., Okay A.I. & Kylander-Clark A.R.C. 2024: Late Neoproterozoic tholeiitic plutonism in Far-East Avalonia (the Dirgine Batholith, Istanbul Zone): exposed mid-crustal section of an oceanic arc. *Precambrian Research* 410, 107475. https://doi.org/10.1016/j.precamres.2024.107475

Yılmazer S., Topuz G., Guillong M., Okay A.I. Demirkaya İ. & Uzun F. 2025: Revealing the early geological history of the Istanbul Zone (far-eastern Avalonia) through zircon U–Pb–Hf isotopic data. *Precambrian Research* 427, 107855. https://doi.org/10.1016/j.precamres.2025.107855

Zabci C., Akyuz H.S & Sunal G. 2003: Istanbul Zonu'nun yapısal evrimine bir yaklaşım: Denizliköy (Gebze) bölgesi. In: Istanbul'un Jeolojisi Sempozyumu (Proceeding of the Symposium on the Geology of the Istanbul Region), İstanbul, p. 2 (in Turkish).

Zlatkin O., Avigad D. & Gerdes A. 2017: The Pelagonian terrane of Greece in the peri-Gondwanan mosaic of the Eastern Mediterranean: Implications for the geological evolution of Avalonia. *Precambrian Research* 290, 163–183. https://doi.org/10.1016/j.precamres.2017.01.005

Zlatkin O., Avigad D. & Gerdes A. 2018: New detrital zircon geochronology from the Cycladic Basement (Greece): Implications for the Paleozoic accretion of peri-Gondwanan terranes to Laurussia. *Tectonics* 37,4679–4699. https://doi.org/10.1029/2018TC005046

Electronic supplementary material is available online:
Supplementary Fig. S1 at https://geologicacarpathica.com/data/files/supplements/GC-76-6-Yilmaz_FigS1.jpg
Supplementary Fig. S2 at https://geologicacarpathica.com/data/files/supplements/GC-76-6-Yilmaz_FigS2.jpg
Supplementary Table S1 at https://geologicacarpathica.com/data/files/supplements/GC-76-6-Yilmaz_TableS1.xlsx
Supplementary Table S2 at https://geologicacarpathica.com/data/files/supplements/GC-76-6-Yilmaz_TableS2.xlsx
Supplementary Table S3 at https://geologicacarpathica.com/data/files/supplements/GC-76-6-Yilmaz_TableS3.xlsx
Supplementary Table S4 at https://geologicacarpathica.com/data/files/supplements/GC-76-6-Yilmaz_TableS4.xlsx